CHAPTER 2

SOLUTIONS OF THE THREE-DIMENSIONAL EQUATIONS

2.01 Introductory

In this chapter we consider solutions of the three-dimensional equations that describe, in closed form, the free vibrations of plates. The aim is to exhibit solutions of the equations for plates with traction-free surfaces; but other boundary conditions are employed, in certain cases, as preliminary steps. Most of the solutions pertain to infinite plates. Those that apply to plates having more than one finite dimension are limited to specific sequences of dimensional ratios. No solutions in closed form have been obtained for unrestricted dimensional ratios of plates with traction-free faces and sides; and none appear to be possible. It is this circumstance which has led to renewed interest in a method of approximation which is the subject of the remaining chapters.

2.02 Simple Thickness-Modes in an Infinite Plate

The plate is bounded by the pair of parallel planes $x_2 = \pm b$ which are termed "faces". Simple thickness-modes are defined as those modes of free vibration in which the faces are traction-free and the components of displacement are independent of the coordinates in the plane of the plate. Thus

$$T_2 = T_4 = T_6 = 0 \quad \text{on} \quad x_2 = \pm b \tag{2.021}$$

$$u_j = u_j(x_2, t) \tag{2.022}$$

In view of (2.022) the strain-displacement relations reduce to

$$\begin{aligned} S_1 &= 0 & S_4 &= \frac{\partial u_2}{\partial x_2} \\ S_2 &= \frac{\partial u_2}{\partial x_2} & S_5 &= 0 \\ S_3 &= 0 & S_6 &= \frac{\partial u_1}{\partial x_2} \end{aligned} \qquad (2.023)$$

A simple thickness-strain (as distinguished from a thickness-strain) is defined as one which is independent of the coordinates x_1 and x_3. There are two types: thickness-stretch (S_2) and thickness-shear (S_4, S_6). The latter two are identified by the designations x_1-simple-thickness-shear (i.e., S_6) and x_3-simple-thickness-shear (i.e., S_4). The simple thickness-stretch is characterized by displacements normal to the faces of the plate and the simple thickness-shears by displacements parallel to the faces of the plate. As will be seen (Sections 2.04 and 2.05) a simple thickness-mode may contain more than one simple thickness-strain.

When the strains are independent of x_1 and x_3, so are the stresses. Hence the stress-equations of motion (1.019), governing simple thickness-modes, reduce to

$$\begin{aligned} \frac{\partial T_6}{\partial x_2} &= \rho \frac{\partial^2 u_1}{\partial t^2} \\ \frac{\partial T_2}{\partial x_2} &= \rho \frac{\partial^2 u_2}{\partial t^2} \\ \frac{\partial T_4}{\partial x_2} &= \rho \frac{\partial^2 u_3}{\partial t^2} \end{aligned} \qquad (2.024)$$

and the components of stress, appearing in these equations, are related to the displacements, according to (1.041) and (2.023), by

$$T_6 = c_{26}\frac{\partial u_2}{\partial x_2} + c_{46}\frac{\partial u_3}{\partial x_2} + c_{66}\frac{\partial u_1}{\partial x_2}$$

$$T_2 = c_{22}\frac{\partial u_2}{\partial x_2} + c_{24}\frac{\partial u_3}{\partial x_2} + c_{26}\frac{\partial u_1}{\partial x_2} \qquad (2.025)$$

$$T_4 = c_{24}\frac{\partial u_2}{\partial x_2} + c_{44}\frac{\partial u_3}{\partial x_2} + c_{46}\frac{\partial u_1}{\partial x_2}$$

Substituting (2.025) in (2.024) we find the differential equations governing the simple thickness-modes:

$$\frac{\partial^2}{\partial x_2^2}(c_{66}u_1 + c_{26}u_2 + c_{46}u_3) = \rho\frac{\partial^2 u_1}{\partial t^2}$$

$$\frac{\partial^2}{\partial x_2^2}(c_{26}u_1 + c_{22}u_2 + c_{24}u_3) = \rho\frac{\partial^2 u_2}{\partial t^2} \qquad (2.026)$$

$$\frac{\partial^2}{\partial x_2^2}(c_{46}u_1 + c_{24}u_2 + c_{44}u_3) = \rho\frac{\partial^2 u_3}{\partial t^2}$$

2.03 Simple Thickness-Modes in an Infinite, Isotropic Plate

When the material of the plate is isotropic,

$$c_{24} = c_{46} = c_{62} = 0$$
$$c_{22} = \lambda + 2\mu \quad , \quad c_{44} = c_{66} = \mu \qquad (2.031)$$

and the equations of motion governing the simple thickness-modes (2.026) reduce to

$$c_j\frac{\partial^2 u_j}{\partial x_2^2} = \rho\frac{\partial^2 u_j}{\partial t^2}, \quad j = 1,2,3 \text{ (no sum)} \qquad (2.032)$$

where

$$c_1 = c_3 = \mu \quad , \quad c_2 = \lambda + 2\mu \qquad (2.033)$$

Assuming a time-factor $e^{i\omega t}$, omitted in the sequel, we find

$$\frac{\partial^2 u_j}{\partial x_2^2} + \eta_j^2 u_j = 0 \tag{2.034}$$

where

$$\eta_j^2 = \rho \omega_j^2 / c_j \tag{2.035}$$

The solutions of (2.034) are

$$u_j = A_j \sin \eta_j x_2 + B_j \cos \eta_j x_2 \tag{2.036}$$

in which A_j and B_j are constants.

The boundary conditions (2.021) reduce, in the isotropic case, to

$$\frac{\partial u_j}{\partial x_2} = 0 \quad \text{on} \quad x_2 = \pm b \tag{2.037}$$

or

$$\pm A_j \eta_j \cos \eta_j b + B_j \eta_j \sin \eta_j b = 0 \tag{2.038}$$

The solutions of (2.038) are

$$B_j = 0, \quad \eta_j = r\pi/2b, \quad r = 1, 3, 5, \ldots \tag{2.039}$$

and

$$A_j = 0, \quad \eta_j = r\pi/2b, \quad r = 2, 4, 6, \ldots \tag{2.0310}$$

Hence

$$\begin{aligned} u_j &= A_j \sin \frac{r\pi x_2}{2b}, \quad r \text{ odd} \\ u_j &= B_j \cos \frac{r\pi x_2}{2b}, \quad r \text{ even} \end{aligned} \tag{2.0311}$$

and the corresponding frequencies are, from (2.035),

$$\omega_j = \frac{r\pi}{2b}\sqrt{\frac{c_i}{\rho}} \tag{2.0312}$$

For convenience, we let $r = p$ for the thickness-stretch modes and $r = q$ for the thickness-shear modes. Then the odd orders of thickness-stretch designate vibrations symmetric with respect to the middle plane of the plate and the even orders of thickness-stretch designate vibrations antisymmetric with respect to the middle plane. Conversely the odd and even orders of thickness-shear are the antisymmetric and symmetric modes, respectively. Thus the frequencies are given by

$$\omega = \frac{p\pi}{2b}\sqrt{\frac{\lambda+2\mu}{\rho}} \begin{cases} p = 1, 3, 5 \ldots\ldots, & \text{(symmetric thickness-stretch)} \\ p = 2, 4, 6 \ldots & \text{(antisymmetric thickness-stretch)} \end{cases} \tag{2.0313}$$

$$\omega = \frac{q\pi}{2b}\sqrt{\frac{\mu}{\rho}} \begin{cases} q = 1, 3, 5 \ldots & \text{(antisymmetric thickness-shear)} \\ q = 2, 4, 6 \ldots\ldots & \text{(symmetric thickness-shear)} \end{cases}$$

The shapes of the first few modes and the associated frequencies are shown in Fig. 2.031 for simple thickness-stretch and in Fig. 2.032 for simple thickness-shear. It will be observed that p or q identifies the number of nodal planes parallel to the faces of the plate.

The antisymmetric mode of lowest frequency is always the thickness-shear mode $q = 1$. The next higher antisymmetric frequency may be that of the first antisymmetric thickness-stretch mode ($p = 2$) or the second antisymmetric thickness-shear mode ($q = 3$), depending on the value of Poisson's ratio. These two modes have the same frequency when $\nu = 1/10$. Generally, Poisson's ratio is greater than $1/10$ so that the second antisymmetric mode is usually the second thickness-shear mode. In any case, the frequency of the second antisymmetric mode is between $2\sqrt{2}$ and 3 times the frequency of the first antisymmetric mode.

In the case of the symmetric modes, the thickness-mode of lowest frequency may be either the first symmetric thickness-stretch mode ($p = 1$) or the

first symmetric thickness-shear mode ($q=2$) according as $\nu \gtrless 1/3$. For values of Poisson's ratio commonly encountered, the frequencies of these two modes may be close together.

Coincidence of frequencies of simple thickness-modes occurs when

$$p^2(\lambda+2\mu) = q^2\mu \tag{2.0314}$$

that is, when

$$\nu = \frac{q^2-2p^2}{2(q^2-p^2)} \tag{2.0315}$$

This phenomenon has an important influence on the character of the frequency spectrum of more general vibrations (see Section 2.11) and, accordingly, affects the formulations and ranges of usefulness of approximate equations of high-frequency vibration of plates (see Chapter 5).

2.04 Simple Thickness-Modes in an Infinite, Monoclinic Plate

When the material of the plate has monoclinic symmetry, with X_1 the two-fold axis, $c_{24}=c_{26}=0$. Then the differential equations (2.026) reduce to

$$\begin{aligned} c_{66}\frac{\partial^2 u_1}{\partial X_2^2} &= \rho\frac{\partial^2 u_1}{\partial t^2} \\ c_{22}\frac{\partial^2 u_2}{\partial X_2^2} + c_{24}\frac{\partial^2 u_3}{\partial X_2^2} &= \rho\frac{\partial^2 u_2}{\partial t^2} \\ c_{24}\frac{\partial^2 u_2}{\partial X_2^2} + c_{44}\frac{\partial^2 u_3}{\partial X_2^2} &= \rho\frac{\partial^2 u_3}{\partial t^2} \end{aligned} \tag{2.041}$$

and, from (2.025), the boundary conditions, on $X_2=\pm b$, reduce to

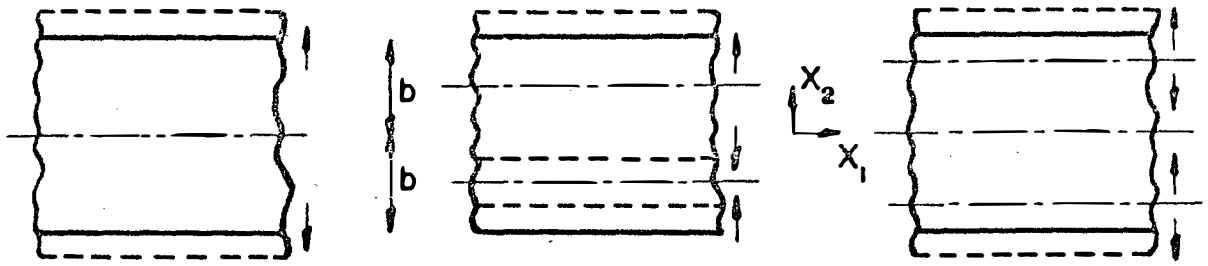

p = 1	p = 2	p = 3
$u_2 = A_2 \sin \frac{\pi x_2}{2b}$	$u_2 = B_2 \cos \frac{\pi x_2}{b}$	$u_2 = A_2 \sin \frac{3\pi x_2}{2b}$
$\omega = \frac{\pi}{2b}\sqrt{\frac{\lambda+2\mu}{\rho}}$	$\omega = \frac{\pi}{b}\sqrt{\frac{\lambda+2\mu}{\rho}}$	$\omega = \frac{3\pi}{2b}\sqrt{\frac{\lambda+2\mu}{\rho}}$
SYMMETRIC	ANTISYMMETRIC	SYMMETRIC

Fig. 2.031

Simple thickness-stretch modes.

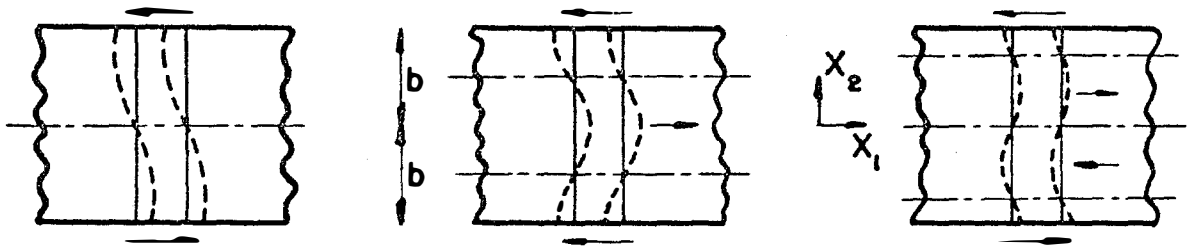

q = 1	q = 2	q = 3
$u_1 = A_1 \sin \frac{\pi x_2}{2b}$	$u_1 = B_1 \cos \frac{\pi x_2}{b}$	$u_1 = A_1 \sin \frac{3\pi x_2}{2b}$
$\omega = \frac{\pi}{2b}\sqrt{\frac{\mu}{\rho}}$	$\omega = \frac{\pi}{b}\sqrt{\frac{\mu}{\rho}}$	$\omega = \frac{3\pi}{2b}\sqrt{\frac{\mu}{\rho}}$
ANTISYMMETRIC	SYMMETRIC	ANTISYMMETRIC

Fig. 2.032

Simple thickness-shear modes.

$$\frac{\partial u_1}{\partial x_2} = 0$$

$$c_{22}\frac{\partial u_2}{\partial x_2} + c_{24}\frac{\partial u_3}{\partial x_2} = 0 \qquad (2.042)$$

$$c_{24}\frac{\partial u_2}{\partial x_2} + c_{44}\frac{\partial u_3}{\partial x_2} = 0$$

Thus, the x_1-thickness-shear strain is not coupled with the other two either in the differential equations or the boundary conditions. Hence the mode shapes and frequencies of x_1-thickness-shear are the same as in the isotropic case (Section 2.03) with the exception that μ is replaced by c_{66}.

To find the shapes and frequencies of the remaining modes, consider solutions of the form

$$u_j = A_j \sin \eta x_2 \, e^{i\omega t} + B_j \cos \eta x_2 \, e^{i\omega t}, \quad j = 2,3. \qquad (2.043)$$

Substituting in the second and third of (2.041), we find

$$\begin{aligned} (c_{22}-c)A_2 + c_{24}A_3 &= 0 \\ c_{24}A_2 + (c_{44}-c)A_3 &= 0 \end{aligned} \qquad (2.044)$$

and

$$\begin{aligned} (c_{22}-c)B_2 + c_{24}B_3 &= 0 \\ c_{24}B_2 + (c_{44}-c)B_3 &= 0 \end{aligned} \qquad (2.045)$$

where

$$c = \rho\omega^2/\eta^2 \qquad (2.046)$$

Thus, modes odd in x_2 are not coupled with modes even in x_2; but thickness-stretch and x_3-thickness-shear are coupled through the constant c_{24}. For a non-vanishing solution, the determinants of (2.044) and (2.045) must vanish:

$$\begin{vmatrix} c_{22}-c & c_{24} \\ c_{24} & c_{44}-c \end{vmatrix} = 0 \qquad (2.047)$$

or

$$2c = c_{22}+c_{44} \pm \sqrt{(c_{22}-c_{44})^2 + 4c_{24}^2} \qquad (2.048)$$

Equations (2.044) and (2.045) also yield the amplitude ratios

$$\frac{A_2}{A_3} = \frac{B_2}{B_3} = \frac{c_{24}}{c-c_{22}} = \frac{c-c_{44}}{c_{24}} \qquad (2.049)$$

The equations from which the frequencies are determined are obtained by substituting (2.043) in the second and third of the boundary conditions (2.042), with the results

$$\begin{matrix} B_j = 0\,, & A_j \cos \eta b = 0 \\ \text{or} & \\ A_j = 0\,, & B_j \sin \eta b = 0 \end{matrix} \qquad (2.0410)$$

These equations have the roots

$$\eta = n\pi/2b \qquad (2.0411)$$

where n is an odd integer for modes odd in x_2 and an even integer for modes even in x_2. Hence, from (2.0411) and (2.046), the frequencies are

$$\omega = \frac{n\pi}{2b}\sqrt{\frac{c}{\rho}} \qquad (2.0412)$$

where the two values of c are given by (2.048).

If the coupling constant c_{24} were zero the two frequencies would be

$$\omega = \frac{n\pi}{2b}\sqrt{\frac{c_{22}}{\rho}}\,, \quad \omega = \frac{n\pi}{2b}\sqrt{\frac{c_{44}}{\rho}} \qquad (2.0413)$$

It may be seen, from (2.048), that the larger of these is raised and the smaller is lowered when $c_{24} \neq 0$.

As an example, we consider the AT cut of quartz, for which $\theta = 35°15'$ (see Fig. 1.041). Then c_{22}, c_{44} and c_{24} in (2.048) are given by the second, fourth and eleventh of (1.046), with $\theta = 35°15'$. Using Mason's values of c°_{pq} as given in (1.047), we find, in units of 10^{10} dyne/cm^2,

$$c_{22} = 129.9 \qquad c_{44} = 39.06 \qquad c_{24} = -5.82 \qquad (2.0414)$$

Then, from (2.048), the two values, say c_2 and c_3, of c are given by

$$\sqrt{\frac{c_2}{c_{22}}} = 1.001 \qquad \sqrt{\frac{c_3}{c_{44}}} = 0.995$$

Thus, due to the coupling, the higher frequency is raised 0.1% and the lower frequency is lowered 0.5%. The mode shapes corresponding to these frequencies may be obtained from (2.043) and (2.049). For example, the modes odd in x_2, with $n=1$, have the shapes

$$\bar{u}_2 = A_2 \sin \frac{\pi x_2}{2b}$$

$$\bar{u}_3 = A_3 \sin \frac{\pi x_2}{2b}$$

$$\frac{A_2}{A_3} = \begin{cases} -15.7, & c = c_2 \\ 0.064, & c = c_3 \end{cases}$$

Thus, in the mode with the higher frequency, the thickness-stretch predominates; whereas, in the mode with the lower frequency, the thickness-shear predominates. The two mode shapes are illustrated in Fig. 2.041.

As noted above, thickness-stretch odd in x_2 couples only with thickness-shear odd in x_2. However, the former is symmetric, whereas the latter is antisymmetric, with respect to the middle plane of the plate. Hence, in a monoclinic plate, symmetric thickness-stretch couples with antisymmetric thickness-shear. It will be seen, later, that this has an important bearing

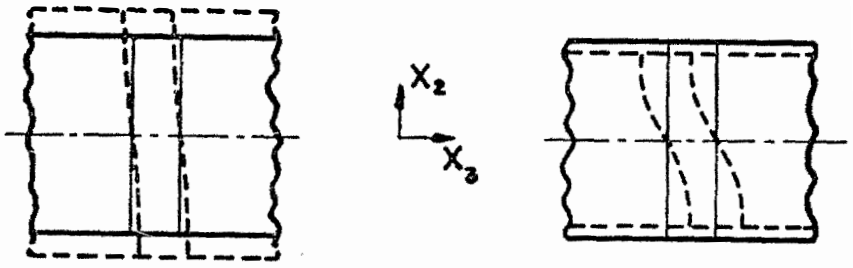

Fig. 2.041

Coupled thickness-stretch and x_3-thickness-shear in a thickness-mode of a monoclinic plate.

on coupling between extensional and flexural vibrations of plates, inasmuch as the former are symmetric, and the latter are antisymmetric, with respect to the middle plane.

2.05 Simple Thickness-Modes in an Infinite, Triclinic Plate

In the case of a plate of general triclinic material, all six elastic constants in (2.025) and (2.026) are non-zero. As a result, all three thickness-strains are coupled in each mode of vibration. By the same procedure as in the preceding section, the frequencies are found to be (Koga, 1932)

$$\omega = \frac{n\pi}{2b}\sqrt{\frac{c}{\rho}} \tag{2.051}$$

where there are three values of c, given by the roots of the cubic equation

$$\begin{vmatrix} c_{66}-c & c_{26} & c_{46} \\ c_{26} & c_{22}-c & c_{24} \\ c_{46} & c_{24} & c_{44}-c \end{vmatrix} = 0 \tag{2.052}$$

2.06 Plane Strain in an Isotropic Body

Let

$$\begin{aligned} u_1 &= u_1(x_1, x_2, t) \\ u_2 &= u_2(x_1, x_2, t) \\ u_3 &= 0 \end{aligned} \tag{2.061}$$

Then we may write, from (1.077)

$$u_1 = \frac{\partial \varphi}{\partial x_1} + \frac{\partial H_3}{\partial x_2}$$
$$u_2 = \frac{\partial \varphi}{\partial x_2} - \frac{\partial H_3}{\partial x_1} \qquad (2.062)$$

where φ and H_3 are independe quations (1.0710) reduce to

(2.063)

— —

The functions

t
t (2.064)

are solutions of (2.063) pr

(2.065)

where prime denotes differe to x_2, and

$$\alpha^2 + \xi^2 = \omega^2/v_1^2$$
$$\beta^2 + \xi^2 = \omega^2/v_2^2$$

Hence

$$f = A \sin \alpha x_2 + B \cos \alpha x_2$$
$$h = C \sin \beta x_2 + D \cos \beta x_2 \qquad (2.067)$$

and

$$
\begin{aligned}
u_1 &= (\xi f + h')\cos\xi x_1\, e^{i\omega t} \\
u_2 &= (f' + \xi h)\sin\xi x_1\, e^{i\omega t} \\
T_{11} &= -\mu[(\beta^2+\xi^2-2\alpha^2)f + 2\xi h']\sin\xi x_1\, e^{i\omega t} \\
T_{22} &= \mu[(\xi^2-\beta^2)f + 2\xi h']\sin\xi x_1\, e^{i\omega t} \\
T_{33} &= -\lambda(\alpha^2+\xi^2)f\sin\xi x_1\, e^{i\omega t} \\
T_{12} &= \mu[2\xi f' + (\xi^2-\beta^2)h]\cos\xi x_1\, e^{i\omega t} \\
u_3 &= T_{23} = T_{31} = 0
\end{aligned}
\tag{2.068}
$$

2.07 Equivoluminal Modes

In the absence of dilatation ($f=0$) the solution (2.068) becomes

$$
\begin{aligned}
u_1 &= h'\cos\xi x_1\, e^{i\omega t} \\
u_2 &= \xi h\sin\xi x_1\, e^{i\omega t} \\
T_{11} &= -T_{22} = -2\mu\xi h'\sin\xi x_1\, e^{i\omega t} \\
T_{12} &= \mu(\xi^2-\beta^2)h\cos\xi x_1\, e^{i\omega t} \\
u_3 &= T_{23} = T_{31} = T_{33} = 0
\end{aligned}
\tag{2.071}
$$

We note that T_{12} vanishes throughout if $\xi^2=\beta^2$, i.e., if

$$\omega = \sqrt{2}\,\xi v_2 = \sqrt{2}\,\beta v_2 \tag{2.072}$$

Then the only remaining requirement for traction-free faces of the plate is $h'=0$ on $x_2=\pm b$. For modes symmetric about the middle plane $x_2=0$,

$$h' = C\beta\cos\beta x_2 \tag{2.073}$$

and, for antisymmetric modes,

$$h' = -D\beta\sin\beta x_2 \tag{2.074}$$

Hence, $T_{22}=0$ on $x_2=\pm b$ if

$$\beta = n\pi/2b \tag{2.075}$$

where n is an odd integer for the symmetric modes and an even integer for the antisymmetric modes. Then, from (2.072), the frequencies are

$$\omega = \frac{n\pi}{2b}\sqrt{\frac{2\mu}{\rho}} \tag{2.076}$$

The complete solutions are, for the symmetric modes (n odd),

$$\begin{aligned} T_{11} &= -T_{22} = -\frac{2\mu n^2\pi^2 C}{4b^2}\sin\frac{n\pi x_1}{2b}\cos\frac{n\pi x_2}{2b}e^{i\omega t} \\ u_1 &= \frac{n\pi C}{2b}\cos\frac{n\pi x_1}{2b}\cos\frac{n\pi x_2}{2b}e^{i\omega t} \\ u_2 &= \frac{n\pi C}{2b}\sin\frac{n\pi x_1}{2b}\sin\frac{n\pi x_2}{2b}e^{i\omega t} \\ u_3 &= T_{23} = T_{31} = T_{33} = T_{12} = 0 \end{aligned} \tag{2.077}$$

and, for the antisymmetric modes (n even),

$$\begin{aligned} T_{11} &= -T_{22} = \frac{2\mu n^2\pi^2 D}{4b^2}\sin\frac{n\pi x_1}{2b}\sin\frac{n\pi x_2}{2b}e^{i\omega t} \\ u_1 &= -\frac{n\pi D}{2b}\cos\frac{n\pi x_1}{2b}\sin\frac{n\pi x_2}{2b}e^{i\omega t} \\ u_2 &= \frac{n\pi D}{2b}\sin\frac{n\pi x_1}{2b}\cos\frac{n\pi x_2}{2b}e^{i\omega t} \\ u_3 &= T_{23} = T_{31} = T_{33} = T_{12} = 0 \end{aligned} \tag{2.078}$$

It may be seen that all planes x_3 = constant are free of traction and planes x_1 = constant and x_2 = constant are traction-free at intervals $2b/n$. Hence the plate breaks up into prisms or plates with traction-free faces. The lengths of the prisms or thicknesses of the plates (in the x_3-direction) are arbitrary since all planes x_3 = constant are free of traction. The cross-sections of the prisms (or the outlines of the plates) are squares of dimension $2b/n$. The displacement of each traction-free face is normal to that face.

The shapes of the first two modes are illustrated in Fig. 2.071.

It may be observed that the frequency of the lowest symmetric thickness-stretch mode is higher than that of the lowest symmetric equivoluminal mode in the ratio $[(\lambda+2\mu)/2\mu]^{1/2}$. However, the frequency of the lowest antisymmetric equivoluminal mode is higher than that of the lowest antisymmetric thickness-mode in the ratio .

The equivoluminal modes described in this section were obtained by Lamé (1866, p. 170). Additional solutions may be obtained by cyclical permutation of the indices. Linear combinations of these solutions describe modes of vibration of a cube (Sommerfeld, 1947).

2.08 Wave-Nature of Equivoluminal Modes

The vibrations described in the preceding section may be shown to be composed of four traveling waves. We consider the antisymmetric modes as an example.

The displacements

$$\begin{aligned} u_1' &= A\cos\theta_1 \sin\gamma(x_1\sin\theta_1 - x_2\cos\theta_1 - v_2 t) \\ u_2' &= A\sin\theta_1 \sin\gamma(x_1\sin\theta_1 - x_2\cos\theta_1 - v_2 t) \\ u_3' &= 0 \end{aligned} \qquad (2.081)$$

constitute a wave of amplitude A and wave-number γ (= 2π/wave-length) whose wave-normal lies in the x_1-x_2-plane, at an angle θ_1 with the x_2-axis (see Fig. 2.081). The direction of the displacement also lies in the x_1-x_2-plane and is at right angles to the wave-normal, i.e., the wave is a shear wave, or equivoluminal wave. It may be verified that the dilatation is zero and the displacements satisfy the equations of motion.

We find, corresponding to (2.081),

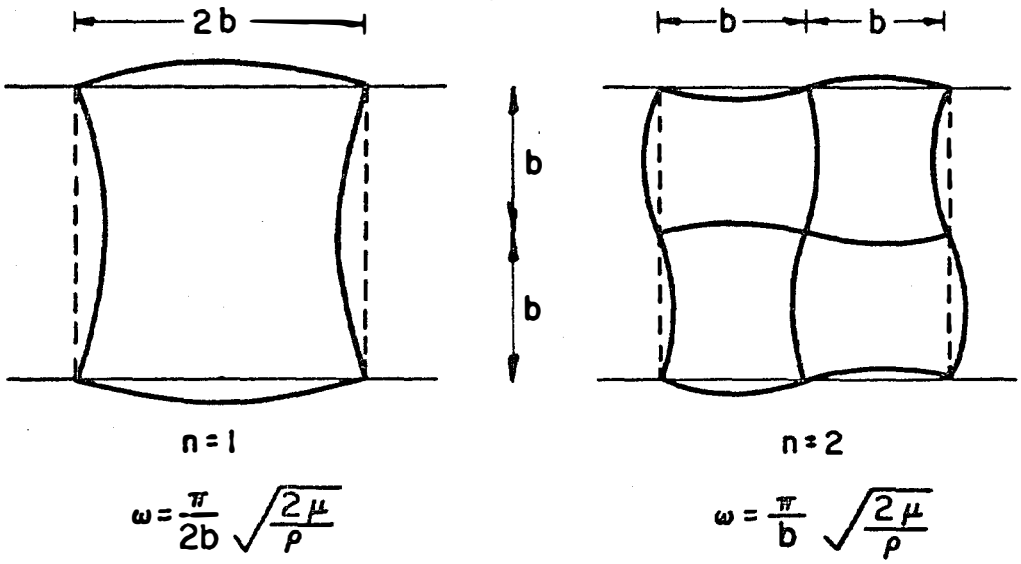

Fig. 2.071

Equivoluminal modes in an isotropic plate.

$$T'_{22} = -A\mu\gamma \sin 2\theta_1 \cos\gamma(x_1 \sin\theta_1 - x_2\cos\theta_1 - v_2 t)$$
$$T'_{12} = -A\mu\gamma \cos 2\theta_1 \cos\gamma(x_1 \sin\theta_1 - x_2\cos\theta_1 - v_2 t) \qquad (2.082)$$

If $\theta_1 = \pi/4$, T'_{12} vanishes throughout and, on $x_2 = \pm b$,

$$T'_{22} = -A\mu\gamma \cos\gamma[\tfrac{1}{2}(x_1 \mp b)\sqrt{2} - v_2 t] \qquad (2.083)$$

Now consider the wave

$$u_1'' = -A\cos\theta_2 \sin\gamma(x_1 \sin\theta_2 + x_2\cos\theta_2 - v_2 t)$$
$$u_2'' = A\sin\theta_2 \sin\gamma(x_1 \sin\theta_2 + x_2\cos\theta_2 - v_2 t)$$
$$u_3'' = 0$$

This is another shear wave in the x_1-x_2-plane (see Fig. 2.082) with amplitude and wave-number as u'. If $\theta_2 = \pi/4$ the wave is at right an u', the stress T''_{12} vanishes and, on $x_2 = \pm b$,

$$T''_{22} = A\mu\gamma \sin\gamma[\tfrac{1}{2}(x_1 \pm b)\sqrt{2} - v_2 t] \qquad (2.084)$$

Superposition of the two waves gives, on $x_2 = \pm b$,

$$T'_{22} + T''_{22} = \pm 2A\mu\gamma \sin\frac{\gamma b}{\sqrt{2}} \cos\gamma\left(\frac{x_1}{\sqrt{2}} - v_2 t\right) \qquad (2.085)$$

Hence, the boundaries $x_2 = \pm b$ are free of traction if

$$\frac{\gamma b}{\sqrt{2}} = \frac{n\pi}{2}, \quad n \text{ even}$$

Thus, if the wave-number satisfies (2.086), the two waves compose wave which travels along the plate by reflecting back and forth between the traction-free planes $x_2 = \pm b$ as shown in Fig. 2.083. As there is also no traction across planes $x_2 = \pm 2bm/n$ (where $m = 0, 1, 2, 3, \ldots$ and $m < n$), the wave traveling along the plate may, equally well, be interpreted as n waves

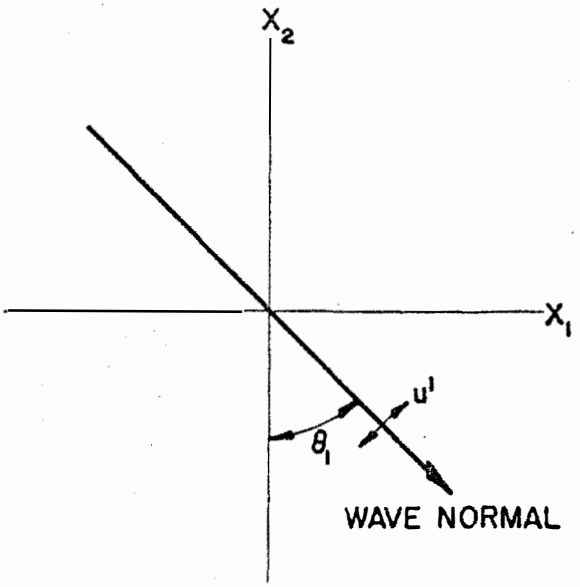

Fig. 2.081

Shear wave u'.

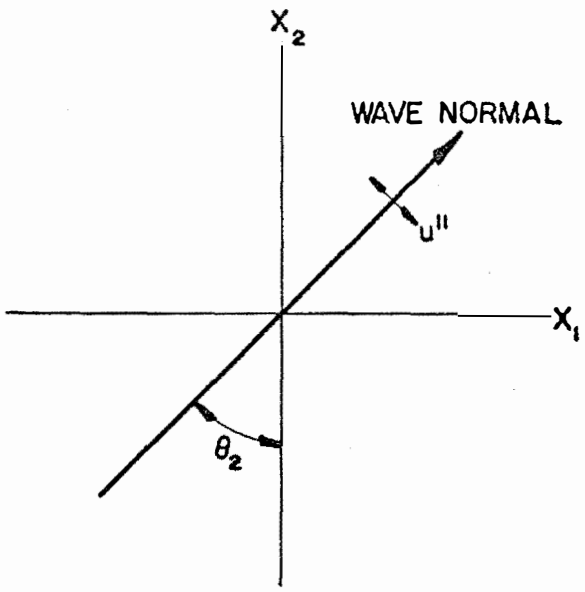

Fig. 2.082

Shear wave u''.

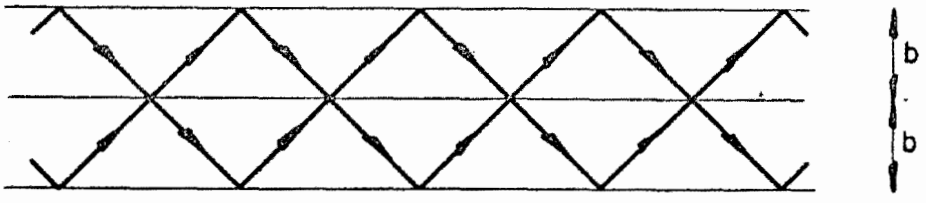

Fig. 2.083

Shear waves $u' + u''$ when $n = 2$.

reflecting between surfaces x_2 = constant, spaced $2b/n$ apart. This is illustrated for $n=2$ in Fig. 2.083.

Now, add another pair of waves identical with u' and u'' but traveling in the reverse directions. The displacements are the same as u' and u'' with v_2 replaced by $-v_2$. The sum of all four displacements gives

$$u_1 = -2\sqrt{2}A\cos\frac{n\pi x_1}{2b}\sin\frac{n\pi x_2}{2b}\cos\gamma v_2 t$$

$$u_2 = 2\sqrt{2}A\sin\frac{n\pi x_1}{2b}\cos\frac{n\pi x_2}{2b}\cos\gamma v_2 t \qquad (2.087)$$

$$u_3 = 0$$

This is the same motion as (2.078) if the amplitude is adjusted and if it is observed that, from (2.086)

$$\gamma v_2 = \frac{n\pi}{2b}\sqrt{\frac{2\mu}{\rho}} = \omega \qquad (2.088)$$

There are no irrotational vibrations analogous to the equivoluminal vibrations of a plate with free faces. This is because a dilatational wave, on reflection at a traction-free surface, always gives rise to an equivoluminal wave (Knott, 1899). Although at most angles of incidence, at a free surface, the shear wave considered in this Section generates a reflected dilatational wave, the angle $\pi/4$ is not one of these.

2.09 Infinite, Isotropic Plate Held between Smooth, Rigid Surfaces (Plane Strain)

From (2.067) and (2.068), we have, for symmetric vibrations,

$$
\begin{aligned}
&f = B\cos\alpha x_2\,, \qquad h = C\sin\beta x_2 \\
&u_1 = (B\xi\cos\alpha x_2 + C\beta\cos\beta x_2)\cos\xi x_1\, e^{i\omega t} \\
&u_2 = (-B\alpha\sin\alpha x_2 + C\xi\sin\beta x_2)\sin\xi x_1\, e^{i\omega t} \\
&T_{22} = \mu[B(\xi^2-\beta^2)\cos\alpha x_2 + 2C\xi\beta\cos\beta x_2]\sin\xi x_1\, e^{i\omega t} \\
&T_{12} = \mu[-2B\xi\alpha\sin\alpha x_2 + C(\xi^2-\beta^2)\sin\beta x_2]\cos\xi x_1\, e^{i\omega t} \\
&u_3 = T_{23} = 0
\end{aligned}
\tag{2.091}
$$

and, for antisymmetric vibrations,

$$
\begin{aligned}
&f = A\sin\alpha x_2\,, \qquad h = D\cos\beta x_2 \\
&u_1 = (A\xi\sin\alpha x_2 - D\beta\sin\beta x_2)\cos\xi x_1\, e^{i\omega t} \\
&u_2 = (A\alpha\cos\alpha x_2 + D\xi\cos\beta x_2)\sin\xi x_1\, e^{i\omega t} \\
&T_{22} = \mu[A(\xi^2-\beta^2)\sin\alpha x_2 - 2D\xi\beta\sin\beta x_2]\sin\xi x_1\, e^{i\omega t} \\
&T_{12} = \mu[2A\xi\alpha\cos\alpha x_2 + D(\xi^2-\beta^2)\cos\beta x_2]\cos\xi x_1\, e^{i\omega t} \\
&u_3 = T_{23} = 0
\end{aligned}
\tag{2.092}
$$

We see that in both cases, except for the modes discussed in Sections 2.02 and 2.07, the conditions $T_{22} = T_{12} = 0$ on $x_2 = \pm b$ impose relations between the dilatational (f) and equivoluminal (h) parts of the solution. That is, the two modes of motion are, in general, coupled through the boundary conditions at traction-free surfaces. There are, however, mixed boundary conditions which do not introduce coupling. For example,

$$
u_2 = 0\,, \quad T_{12} = 0 \quad \text{on} \quad x_2 = \pm b \tag{2.093}
$$

i.e., no normal displacement and no tangential traction. These conditions may be visualized by imagining the plate to be held between perfectly smooth, rigid, plane surfaces. Although the conditions cannot be realized physically, they are of interest as a starting point for the study of the development of coupling to the full coupling associated with traction-free boundaries. No

normal traction and [illegible] are conditions which could also be used for thi[illegible]

On substituti[illegible] (2.091) and (2.092) in (2.093), we find that the lat[illegible] symmetric modes, if

[illegible] or (2.094)

and, for the antisym[illegible]

[illegible] or (2.095)

Thus, for bot[illegible] latational and equi[illegible] motions can exist in

$$\alpha = m\pi/2b \ ,$$

where m and n are ev[illegible] ic modes and odd in[illegible] the antisymmetric mo[illegible] 096) yield the freq[illegible] vibration of the dil[illegible]

$$\frac{\omega}{\omega_\alpha} = \sqrt{\left(\frac{m\pi}{\quad}\right)^2}$$

and the equivolumina[illegible]

$$\frac{\omega}{\omega_\alpha} = \frac{\omega_\beta}{\omega_\alpha}\sqrt{\frac{\quad}{\quad}}$$

where

$$\frac{2\pi}{\Lambda}\sqrt{\frac{+2\mu}{\rho}}$$

$$p - \tfrac{1}{2}V_2 - \frac{2\pi}{}\sqrt{\mu} \qquad (2.099)$$

in which Λ $(=2\pi/\xi)$ is the wave-length in the x_1-direction. The reference frequencies ω_α and ω_β are the frequencies of the fundamental thickness-stretch and thickness-shear modes, respectively, that would be found in a free plate whose thickness is equal to the distance between nodes along the x_1-direction in the plate supported between smooth, rigid planes.

The frequency ratios (2.097) and (2.098) are plotted against ξb (i.e., $2\pi b/\Lambda$), in Fig. 2.091, for $\omega_\beta/\omega_\alpha = 1/2$, i.e., $\lambda = 2\mu$, i.e., $\nu = 1/3$. Curves m= constant, n = constant give the frequencies of the dilatational and equivoluminal modes, respectively; m and n even are for symmetric modes, while m and n odd are for antisymmetric modes. Since ξ (the wave-number in the x_1-direction) appears in both ordinate and abscissa, the curves are best interpreted by considering that they give the change in frequency as the thickness $(2b)$ varies, while ξ is held constant.

Considering, now, the variation of frequency with ξ, while b remains constant, we note, from (2.097) and (2.098), that as $\xi b \to 0$, the limiting frequencies are those of the simple thickness-modes given by (2.0312). This becomes apparent if (2.097) and (2.098) are rewritten as

$$\frac{\omega}{\omega_s} = c\sqrt{m^2 - \left(\frac{2\xi b}{\pi}\right)^2} \qquad (2.0910)$$

$$\frac{\omega}{\omega_s} = \sqrt{n^2 + \left(\frac{2\xi b}{\pi}\right)^2} \qquad (2.0911)$$

for the dilatational and equivoluminal modes, respectively, where

$$c = \sqrt{\frac{\lambda+2\mu}{\mu}} = \sqrt{\frac{2(1-\nu)}{1-2\nu}} \qquad (2.0912)$$

$$\omega_s = \frac{\pi}{2b}\sqrt{\frac{\mu}{\rho}} \qquad (2.0913)$$

i.e., c is the ratio of the velocity of dilatational to equivoluminal waves

in an infinite body and ω_s is the frequency of the lowest, simple thickness-shear mode.

Equations (2.0910) and (2.0911) are plotted in Fig. 2.092 for three values of Poisson's ratio. The curves n = constant, representing the frequencies of the equivoluminal modes, remain fixed as Poisson's ratio changes; but the curves m = constant, representing the dilatational modes, spread upwards as Poisson's ratio increases.

It should be observed that the frequencies of the antisymmetric dilatational modes ($m=1,3,5,\ldots$) approach, in the limit $\zeta b = 0$, the frequencies of the symmetric, simple thickness-stretch modes ($p=1,3,5,\ldots$) and the frequencies of the symmetric dilatational modes ($m=2,4,6,\ldots$) approach the frequencies of the antisymmetric, simple thickness-stretch modes ($p=2,4,6,\ldots$). On the other hand, the frequencies of the antisymmetric ($n=1,3,5,\ldots$) and the symmetric ($n=2,4,6,\ldots$) equivoluminal modes approach the frequencies of the antisymmetric ($q=1,3,5,\ldots$) and symmetric ($q=2,4,6,\ldots$) simple thickness-shear modes, respectively. This is because the boundary conditions (2.093) for smooth, rigid surfaces are satisfied by the simple thickness-shear modes but not by the simple thickness-stretch modes.

2.10 Infinite, Isotropic Plate Held between Smooth, Elastic Surfaces (Plane Strain)

The effect of a gradual relaxation of the constraint on the faces of the plate may be studied by considering linearly elastic springs to be uniformly distributed between the plate and the rigid surfaces. Then the boundary conditions are

$$T_{22} = \mp k u_2 \,, \quad T_{12} = 0 \qquad \text{on} \quad x_2 = \pm b \tag{2.101}$$

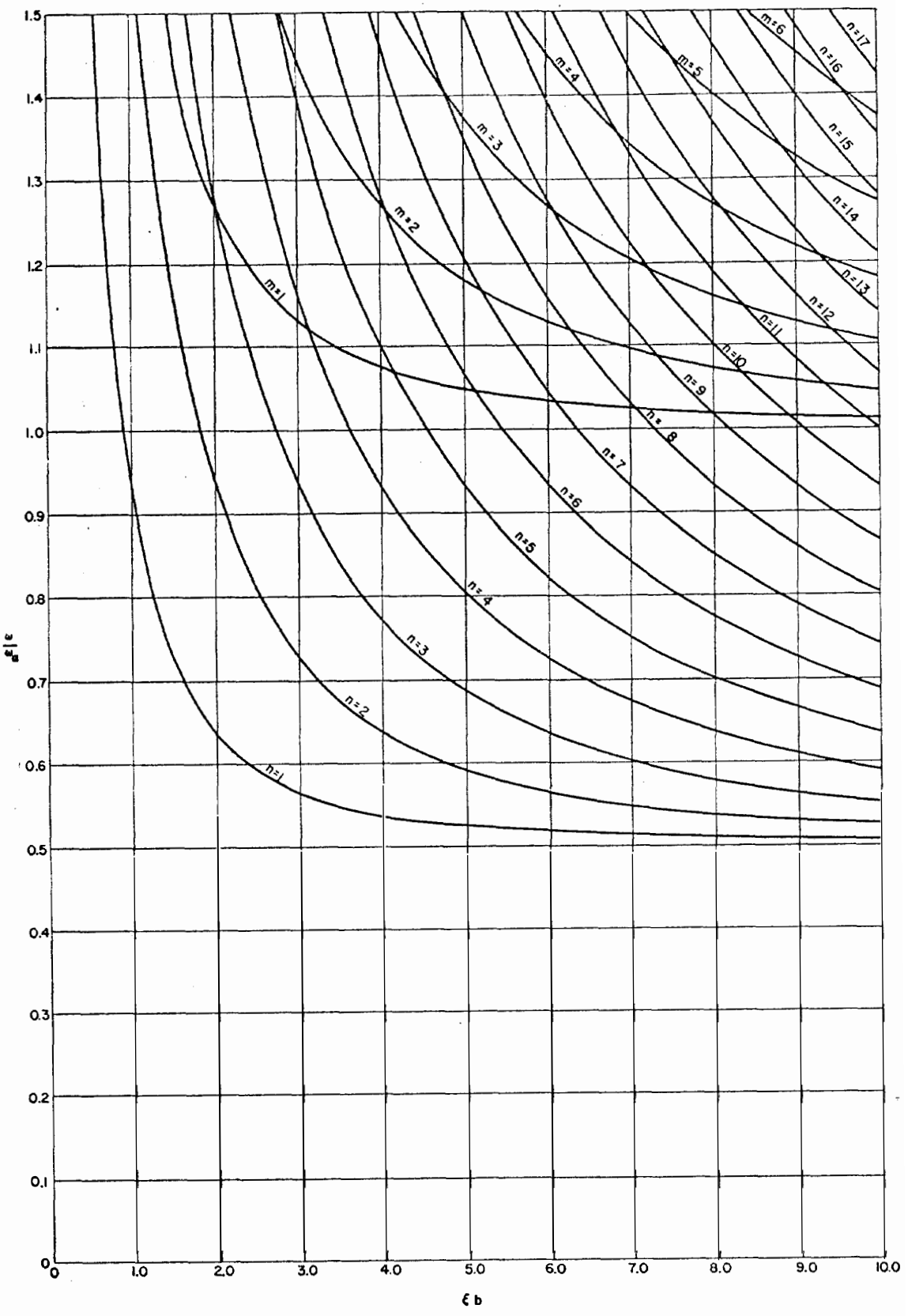

Fig. 2.091

Frequency spectrum of uncoupled dilatational and equivoluminal modes of vibration of an infinite, isotropic plate held between smooth, rigid surfaces. (Poisson's ratio = 1/3)

where k is the spring constant. When the springs are infinitely hard ($k=\infty$) the boundary conditions revert back to (2.093). When the springs are infinitely soft ($k=0$), the faces are traction-free.

From (2.091) and (2.092), the boundary conditions become, for the symmetric modes,

$$\begin{aligned} \mu[B(\xi^2-\beta^2)\cos\alpha b + 2C\xi\beta\cos\beta b] &= k(B\alpha\sin\alpha b - C\xi\sin\beta b) \\ 2B\xi\alpha\sin\alpha b - C(\xi^2-\beta^2)\sin\beta b &= 0 \end{aligned} \tag{2.102}$$

and, for the antisymmetric modes,

$$\begin{aligned} \mu[A(\xi^2-\beta^2)\sin\alpha b - 2D\xi\beta\sin\beta b] &= -k(A\alpha\cos\alpha b + D\xi\cos\beta b) \\ 2A\xi\alpha\cos\alpha b + D(\xi^2-\beta^2)\cos\beta b &= 0 \end{aligned} \tag{2.103}$$

To obtain these conditions, the frequency and x_1-wave-length of the dilatational part must be set equal to the frequency and x_1-wave-length of the equivoluminal part, in order for the conditions to hold for all x_1 and t. It is apparent, from (2.102) and (2.103) that, if $0 \ll k < \infty$ and $\xi b \neq 0$, the equivoluminal and dilatational motions are coupled.

Considering the antisymmetric modes, we observe that (2.103) are satisfied by

$$\begin{aligned} \cos\alpha b = 0, \quad \cos\beta b = 0 \\ \frac{A}{D} = \pm\frac{2\xi\beta}{\xi^2-\beta^2} \end{aligned} \tag{2.104}$$

Recalling (2.095), we see that (2.103) have some roots which give the same frequencies that were obtained for the case of smooth, rigid surfaces. Since, now, ξ and ω must be the same for both the dilatational and equivoluminal parts, these roots determine frequencies and wave-numbers which fall on the curves in Fig. 2.091 only at the intersections of curves m odd, n odd. Inasmuch as the replacement of the rigid surface by an elastic one

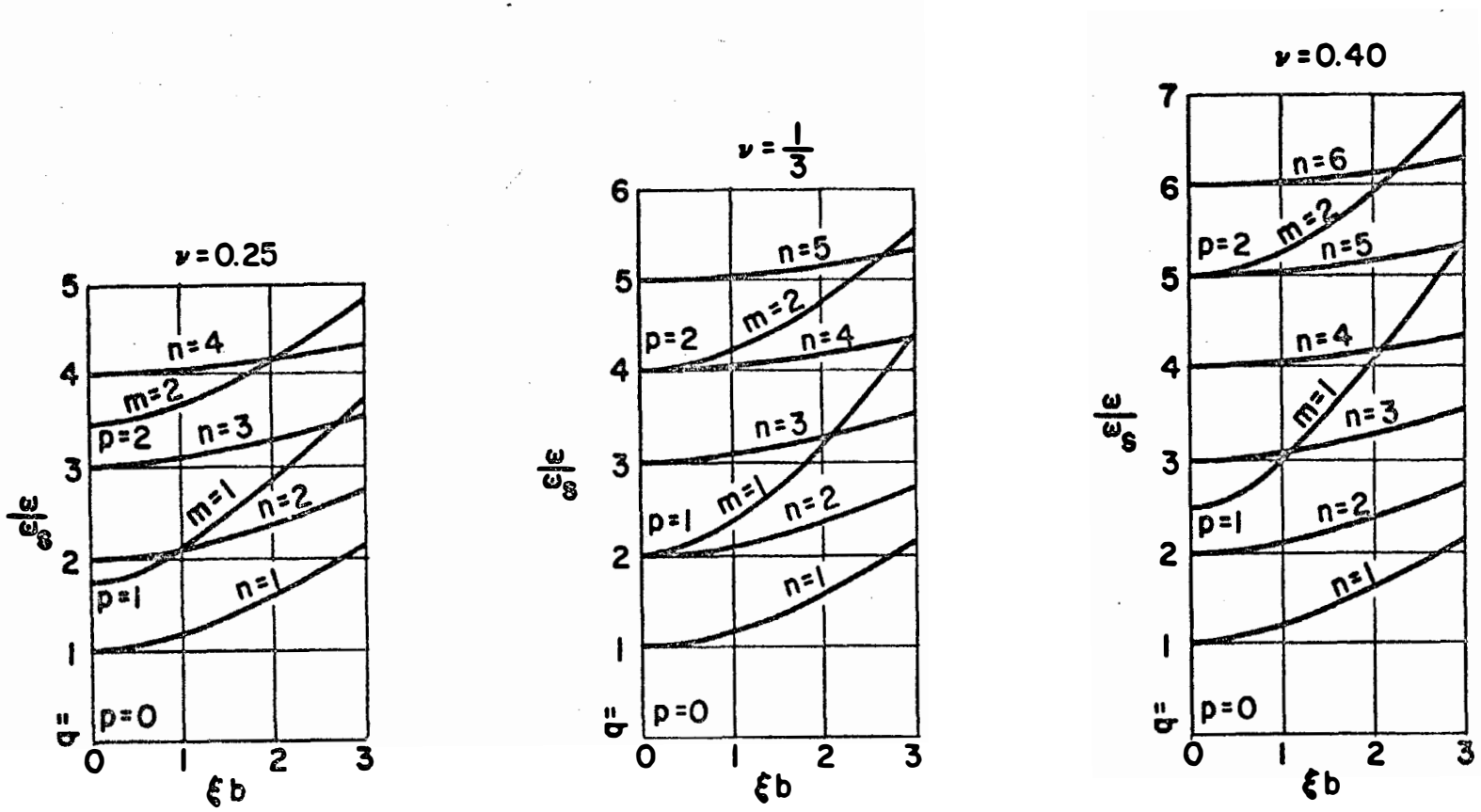

Fig. 2.092

Influence of Poisson's ratio on frequencies of uncoupled dilatational and equivoluminal modes of vibration of an infinite, isotropic plate held between smooth, rigid surfaces.

is a relaxation of a constraint, the frequencies between intersection points are lower in the latter case. Also, for $k>0$, $\sin\alpha b=0$, $\sin\beta b=0$ is not a solution of (2.103), hence the frequency curves for the elastically supported plate do not pass through the intersections of curves m even, n even in Fig. 2.091. These considerations permit us to sketch the frequency spectrum as the spring stiffness diminishes. A portion of the spectrum is illustrated in Fig. 2.101. The two dashed curves marked $0<k<\infty$ are for successive values of k, the lower curve corresponding to the smaller value. When $k=0$, the curve representing the frequencies of the coupled motions passes through the intersections of m even, n even, in addition to the intersections m odd, n odd, since $\sin\alpha b=0$ and $\sin\beta b=0$ are then solutions of (2.103).

The situation is very similar for the symmetric coupled modes. It is only necessary to interchange sine and cosine, odd and even in the preceding exposition.

Turning, now, to the long wave-length end of the spectrum, we note that in the limit, as $\xi b\to 0$,

$$\alpha=\eta_2\ ,\quad \beta=\eta_1\ ,\quad \mu(\xi^2-\rho^2)=(\lambda+2\mu)\eta_2^2$$
$$\omega=\eta_1\sqrt{\frac{\mu}{\rho}}\ ,\quad \omega=\eta_2\sqrt{\frac{\lambda+2\mu}{\rho}} \tag{2.105}$$

where η_1 and η_2 are the wave-numbers of the displacements u_1 and u_2, respectively (see Section 2.03). Then (2.102), for the symmetric modes, becomes

$$B(\lambda+2\mu)\eta_2\cos\eta_2 b=Bk\sin\eta_2 b$$
$$C\sin\eta_1 b=0 \tag{2.106}$$

and (2.103), for the antisymmetric modes, becomes

$$A(\lambda+2\mu)\eta_2\sin\eta_2 b=-Ak\cos\eta_2 b$$
$$D\cos\eta_1 b=0 \tag{2.107}$$

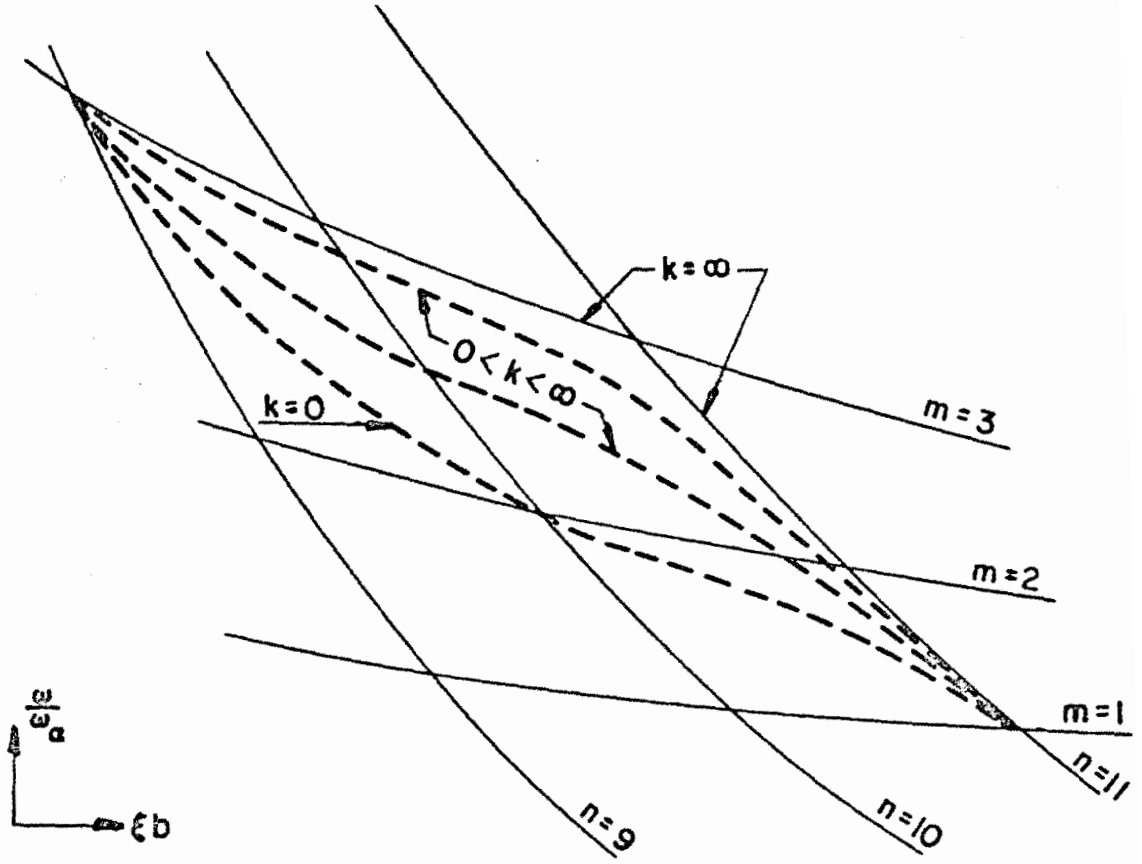

Fig. 2.101

Effect, on the frequency spectrum of antisymmetric modes, of the development of coupling between dilatational and equivoluminal modes as a result of relaxation of boundary constraint.

Thus the dilatational and equivoluminal modes are no longer coupled.

The equivoluminal modes have become identical with the simple thickness-shear modes (Section 2.03) with

$$\omega = \frac{n\pi}{2b}\sqrt{\frac{\mu}{\rho}} = \frac{q\pi}{2b}\sqrt{\frac{\mu}{\rho}} \tag{2.108}$$

where n or q is odd for the antisymmetric modes and even for the symmetric modes. Since the frequencies are independent of k, the ordinates, at $\xi b = 0$, of the curves n = constant, in Fig. 2.092, do not change as k is varied.

The frequencies of the dilatational modes have become

$$\omega = \frac{(\eta_2 b)}{b}\sqrt{\frac{\lambda+2\mu}{\rho}} \tag{2.109}$$

where $(\eta_2 b)$ are the roots of

$$\tan(\eta_2 b) = -\frac{(\eta_2 b)(\lambda+2\mu)}{kb} \tag{2.1010}$$

for the symmetric modes and

$$\cot(\eta_2 b) = \frac{(\eta_2 b)(\lambda+2\mu)}{kb} \tag{2.1011}$$

for the antisymmetric modes. As $k \to \infty$, the roots approach

$$\eta_2 b = \frac{m\pi}{2} \tag{2.1012}$$

where m is even for the symme and odd for the antisymmetric modes. The corresponding frequencies by the ordinates, at $\xi b = 0$, of the curves m = constant in Fig. 2 $\to 0$, the roots approach

$$\eta_2 b = \frac{p\pi}{2} \tag{2.1013}$$

where p is <u>odd</u> for the symmetric modes and <u>even</u> for the antisymmetric modes.

The corresponding frequencies are those of the simple thickness-stretch modes and are given by the points marked $p=0,1,2,\ldots$ in Fig. 2.092. As k diminishes from infinity to zero, the ordinates, at $\xi b=0$, drop. For example, referring to Fig. 2.092(a) the curve for the symmetric mode which starts out as $m=2$ at $k=\infty$, (for which the figure is drawn) descends in the spectrum until its ordinate, at $\xi b=0$, reaches the point marked $p=1$ when $k=0$. The whole curve distorts in the process and ends up as the heavy full line which is the second from the bottom in Fig. 2.113(a). Similarly, the curve for the antisymmetric mode, which starts out as $m=1$ in Fig. 2.092, descends in the spectrum until its ordinate, at $\xi b=0$, is zero. Its limiting shape, at $k=0$, is given by the lowest dashed line in Fig. 2.113(a). Meanwhile, the curves marked $n=2$ and $n=1$, while retaining their ordinates at $\xi b=0$, shift their positions to the third, heavy, full line and the second dashed line, respectively, in Fig. 2.113(a).

During the passage from $k=\infty$ to $k=0$ the mode-shapes (i.e., the variation of displacement with x_2) do not change, in the case of the equivoluminal modes, when $\xi b=0$, since the boundary conditions are independent of k. The mode-shapes of the dilatational modes, however, depend on k. When $\xi b=0$, the dilatational modes involve only the component of displacement u_2. This has nodes or antinodes at $x_2=\pm b$ according as k is infinity or zero. At intermediate values of k there are neither nodes or antinodes at the surfaces. The shape of the lowest antisymmetric mode is of special interest. Here the displacement is proportional to $\cos\eta_2 b$ where $\eta_2 b$ is the lowest root of (2.1011). When $k=\infty$, $\eta_2 b=\pi/2$ (i.e., $m=1$) so that the displacement varies as a half-sine wave through the thickness, with a node at each surface and the maximum at the center. As k diminishes, so does the first root of (2.1011). Hence the nodes spread outward from the surfaces of the plate, leaving a displacement, inside the plate, which approaches a uniform distribution across the

thickness as k approaches zero. Meanwhile the frequency, which is proportional to $\eta_2 b$, has also diminished and is approaching the lowest dashed line in Fig. 2.113(a). This mode, then, is the one which contributes the uniform part of the transverse displacement accompanying low-frequency flexural vibrations of plates.

It is to be noted that (2.1011) has a root $\eta_2 b=0$ only when $k=0$. On the other hand, (2.1010), which governs the frequencies of the symmetric modes, always has a root $\eta_2 b=0$. Hence there is always present a mode whose limiting frequency, at $\xi b=0$, is zero. Similarly, there is a zero-root of the second of (2.106), governing the symmetric thickness-shear modes. This accounts for the presence of the lowest, heavy, full curve, in Fig. 2.113(a), despite the fact that the next higher symmetric dilatational mode, which starts out, at $k=\infty$, as the curve $m=2$ in Fig. 2.092(a), never falls below the point $p=1$ at $\xi b=0$.

2.11 Coupled Dilatational and Equivoluminal Modes in an Infinite, Isotropic Plate with Free Faces (Plane Strain)

We come, now, to the problem of the vibrations, in a state of plane strain, of a plate with traction-free faces (Rayleigh, 1889). The boundary conditions are obtained from (2.102) and (2.103) by setting $k=0$, with the results, for the symmetric modes,

$$\begin{aligned} B(\xi^2-\beta^2)\cos\alpha b + 2C\xi\beta\cos\beta b &= 0 \\ 2B\xi\alpha\sin\alpha b - C(\xi^2-\beta^2)\sin\beta b &= 0 \end{aligned} \qquad (2.111)$$

and, for the antisymmetric modes,

$$\begin{aligned} A(\xi^2-\beta^2)\sin\alpha b - 2D\xi\beta\sin\beta b &= 0 \\ 2A\xi\alpha\cos\alpha b + D(\xi^2-\beta^2)\cos\beta b &= 0 \end{aligned} \qquad (2.112)$$

These equations have the four solutions

$$\begin{aligned} &B=0,\ \xi=0,\ \sin\beta b=0\\ &C=0,\ \xi=0,\ \cos\alpha b=0\\ &A=0,\ \xi=0,\ \cos\beta b=0\\ &D=0,\ \xi=0,\ \sin\alpha b=0 \end{aligned} \tag{2.113}$$

which lead to the simple thickness-modes discussed in Section 2.03. Equations (2.111) and (2.112) also have the two solutions

$$\begin{aligned} &B=0,\ \xi^2=\beta^2,\ \cos\beta b=0\\ &A=0,\ \xi^2=\beta^2,\ \sin\beta b=0 \end{aligned} \tag{2.114}$$

which lead to the equivoluminal modes discussed in Section 2.07. Finally, (2.111), governing the symmetric motions, have the solution

$$\frac{B}{C}=-\frac{2\xi\beta\cos\beta b}{(\xi^2-\beta^2)\cos\alpha b} \tag{2.115}$$

$$\frac{\tan\beta b}{\tan\alpha b}=-\frac{4\xi^2\alpha\beta}{(\xi^2-\beta^2)^2} \tag{2.116}$$

and (2.112), governing the antisymmetric motions, have the solution

$$\frac{A}{D}=\frac{2\xi\beta\sin\beta b}{(\xi^2-\beta^2)\sin\alpha b} \tag{2.117}$$

$$\frac{\tan\beta b}{\tan\alpha b}=-\frac{(\xi^2-\beta^2)^2}{4\xi^2\alpha\beta} \tag{2.118}$$

These solutions, first obtained by Rayleigh in 1889, have been the subject of extensive study in the ensuing years (see, for example, Lamb, 1917 and Holden, 1951). The frequency spectra determined by (2.116) and (2.118) are illustrated in Fig. 2.111 for $\lambda=2\mu$, i.e., $\nu=1/3$. The full lines are for the symmetric modes and the dashed lines are for the

antisymmetric modes. We proceed to a detailed analysis of the frequencies.

Now,

$$\alpha = \xi\sqrt{\frac{\omega^2}{\omega_\alpha^2} - 1}$$
$$\beta = \xi\sqrt{\frac{\omega^2}{\omega_\beta^2} - 1} \qquad (2.119)$$

where ω_α and ω_β are defined by (2.099). In an infinite plate ξ must be real. Hence α is real if $\omega > \omega_\alpha$ and imaginary if $\omega < \omega_\alpha$; β is real if $\omega > \omega_\beta$ and imaginary if $\omega < \omega_\beta$. Recalling that $\omega_\alpha > \omega_\beta$ we see that there are three ranges of frequencies

$$\omega < \omega_\beta, \quad \alpha \text{ and } \beta \text{ imaginary}$$
$$\omega_\beta < \omega < \omega_\alpha, \quad \alpha \text{ imaginary, } \beta \text{ real}$$
$$\omega > \omega_\alpha, \quad \alpha \text{ and } \beta \text{ real}$$

in which the roots of (2.116) and (2.118) (and also the mode-shapes) will have different characters since the transcendental functions of α and β will be trigonometric or hyperbolic according as α and β are real or imaginary. When α or β is imaginary we shall let $\alpha = i\alpha_1$ or $\beta = i\beta_1$ where α_1 and β_1 are real.

In the lowest frequency range ($\omega < \omega_\beta$), equation (2.116), for the symmetric modes, becomes (since $\tan iz = i\tanh z$)

$$\frac{\tanh \beta_1 b}{\tanh \alpha_1 b} = \frac{4\xi^2\alpha_1\beta_1}{(\xi^2+\beta_1^2)^2} \qquad (2.1110)$$

and equation (2.118), for the antisymmetric modes, becomes

$$\frac{\tanh \beta_1 b}{\tanh \alpha_1 b} = \frac{(\xi^2+\beta_1^2)^2}{4\xi^2\alpha_1\beta_1} \qquad (2.1111)$$

For very short wave-lengths along x_1, $\xi b \to \infty$, $\alpha_1 b \to \infty$ and $\beta_1 b \to \infty$. Hence, both (2.1110) and (2.1111) reduce to

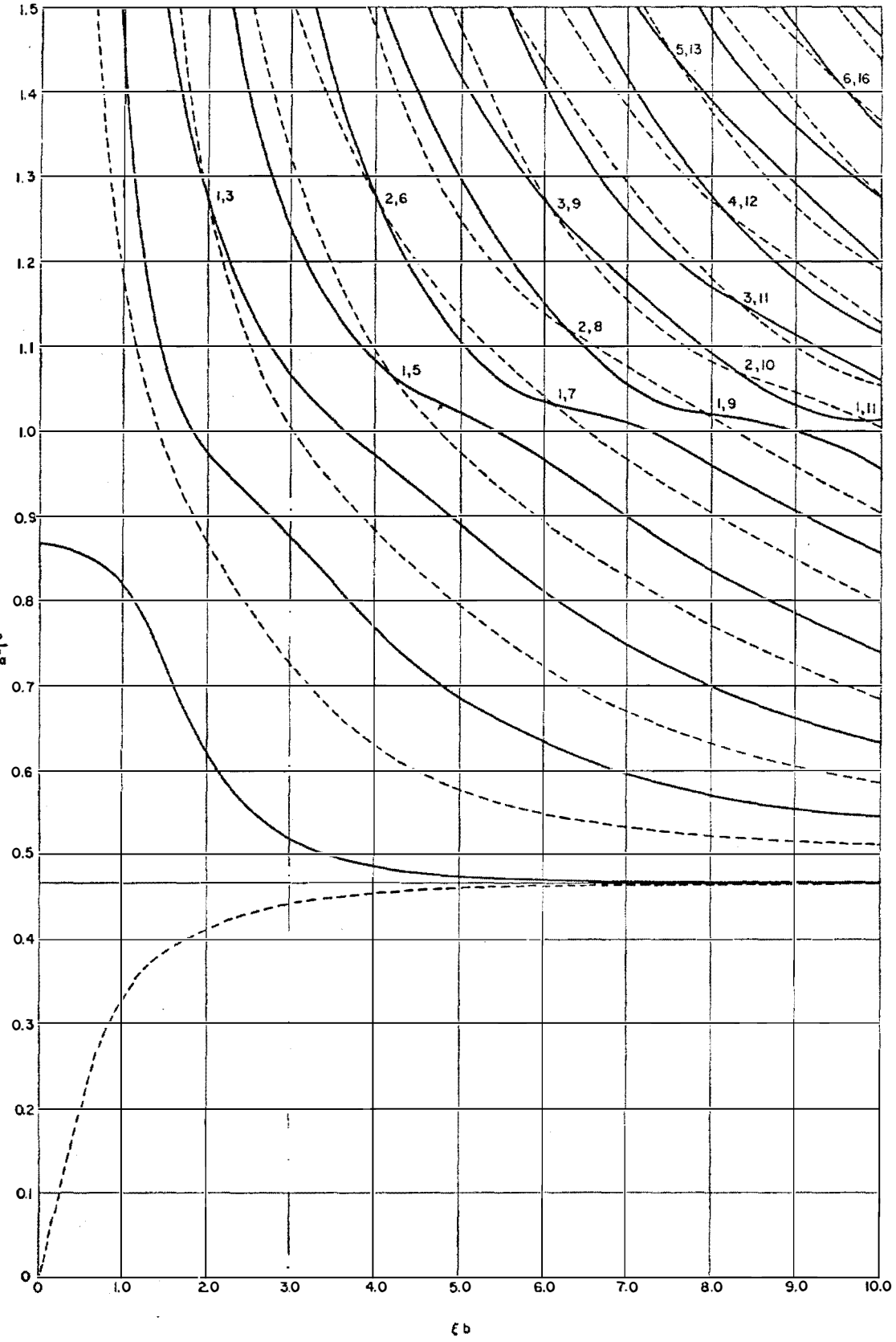

Fig. 2.111

Frequency spectrum of coupled equivoluminal and dilatational modes of vibration of an infinite, isotropic plate with free faces.

$$(\xi^2+\beta_1^2)^2-4\xi^2\alpha_1\beta_1=0 \tag{2.1112}$$

or

$$\frac{\omega^2}{\omega_\beta^2}\left[\frac{\omega^6}{\omega_\beta^6}-8\frac{\omega^4}{\omega_\beta^4}+8\left(3-2\frac{\omega_\beta^2}{\omega_\alpha^2}\right)\frac{\omega^2}{\omega_\beta^2}-16\left(1-\frac{\omega_\beta^2}{\omega_\alpha^2}\right)\right]=0 \tag{2.1113}$$

which is the equation governing the frequency of surface-waves (Rayleigh, 1887). This equation has only one root in the range $0<\omega<\omega_\beta$. For $\nu=1/3$, $\omega/\omega_\beta=0.932$ and, since $\omega_\beta/\omega_\alpha=\frac{1}{2}$, $\omega/\omega_\alpha=0.466$. This is the asymptotic value of the two lowest curves in Fig. 2.111.

For very long wave-lengths along x_1, $\xi b\to 0$, $\alpha b\to 0$, $\beta b\to 0$. At this limit, equation (2.1110) has no root in the range $0<\omega<\omega_\beta$. As for (2.1111), for the antisymmetric motion, we write

$$\begin{aligned}\tanh\alpha_1 b &\simeq \alpha_1 b\left(1-\tfrac{1}{3}\alpha_1^2 b^2\right)\\ \tanh\beta_1 b &\simeq \beta_1 b\left(1-\tfrac{1}{3}\beta_1^2 b^2\right)\end{aligned} \tag{2.1114}$$

and find

$$\frac{\omega}{\omega_\beta}=2\xi b\sqrt{\frac{1}{3}\left(1-\frac{\omega_\beta^2}{\omega_\alpha^2}\right)} \tag{2.1115}$$

on the supposition that ω/ω_β is small, which is seen to be verified. For $\nu=1/3$, (2.1115) may be written $\omega/\omega_\alpha=\xi b/2$. This gives the initial slope of the lowest curve in Fig. 2.111. Equation (2.1115) may be written as

$$\omega=\xi^2 b\sqrt{\frac{E}{3\rho(1-\nu^2)}} \tag{2.1116}$$

which is the familiar form in the classical theory of flexure of thin plates.

In the intermediate range of frequencies ($\omega_\beta<\omega<\omega_\alpha$) we write, for the symmetric modes,

$$\frac{\tan\beta b}{\tanh\alpha_1 b}=\frac{4\xi^2\alpha_1\beta}{(\xi^2-\beta^2)^2} \tag{2.1117}$$

and, for the antisymmetric r

$$\text{———} - \frac{(\xi^2-\beta^2)^2}{4\xi^2\alpha_1\beta} \qquad (2.1118)$$

Equation (2.1117) ha cy in this range as $\xi b \to 0$. Noting that the limit of th $b \to 0$, is β/α_1 , we have

$$(\xi^2-\beta^2)^2 = 4\xi^2\alpha_1^2 \qquad (2.1119)$$

or

$$\frac{\omega}{\omega_\alpha} = \frac{2\omega_\beta}{\omega_\alpha}\sqrt{1-\frac{\omega_\beta^2}{\omega_\alpha^2}} \qquad (2.1120)$$

For $\nu = 1/3$, $\omega_\alpha/\omega_\beta = 2$ so that c is is the ordinate, at $\xi b = 0$, of the curve for the lowest ig. 2.111. Equation (2.1120) may be written as

$$\omega = \xi\sqrt{\frac{E}{\rho(1-\nu^2)}} \qquad (2.1121)$$

which is the familiar form the classical theory of extensional vibrations of thi

The curve for the lo is the only one that crosses the boundary between the lo nges. The cross-over point is found by taking the limi >0 , with the result

$$2\tanh\alpha_1 b = (1-\nu)\alpha_1 b \qquad (2.1122)$$

Then the abscissa of the cr

$$\alpha_1 b\sqrt{2(1-\nu)} \qquad (2.1123)$$

where $\alpha_1 b$ is the root of (2. $\alpha_1 b = 2.99$ and $\xi b = 3.4$ shown in Fig. 2.111.

The curves for all the higher modes approach ω_b/ω_α ($= 1/2$ for $\nu = 1/3$)

asymptotically as $\S b \to \infty$. That is, except for the first symmetric and first antisymmetric modes, $\omega \to \omega_\beta$ as the wave-length approaches zero.

In the highest range of frequencies ($\omega > \omega_\alpha$) we use (2.116) and (2.118), since both α and β are real. Both equations have the special roots

$$\sin \alpha b = 0 \ , \quad \sin \beta b = 0 \ , \quad \cos \alpha b = 0 \ , \quad \cos \beta b = 0$$

so that the frequency curves for both symmetric and antisymmetric modes pass through the intersections of curves m odd, n odd and also m even, n even of Fig. 2.091, in the manner indicated by the curve $k = 0$ in Fig. 2.101 for the antisymmetric modes. With this information and with the results of the analysis of limiting cases given above, the frequency spectrum of ω/ω_α vs. $\S b$ may be sketched approximately, following the pattern indicated in Fig. 2.101.

For detailed calculations of intermediate points, it is convenient to alter the form of the transcendental equations.

Let

$$a = \beta/\alpha \ , \quad \gamma = \alpha b \tag{2.1124}$$

Then

$$a = \sqrt{\frac{c^2 \frac{\omega^2}{\omega_\alpha^2} - 1}{\frac{\omega^2}{\omega_\alpha^2} - 1}} \tag{2.1125}$$

$$\S b = \gamma \sqrt{\frac{a^2 - c^2}{c^2 - 1}} \tag{2.1126}$$

where $c = \omega_\alpha/\omega_\beta$. With (2.1124), the equations (2.116) and (2.118), for the symmetric and antisymmetric modes, respectively, become

$$\frac{\tan a\gamma}{\tan \gamma} = -\frac{4a(c^2-1)(a^2-c^2)}{[a^2-c^2-a^2(c^2-1)]^2}$$

$$\frac{\tan a\gamma}{\tan \gamma} = -\frac{[a^2-c^2-a^2(c^2-1)]^2}{4a(c^2-1)(a^2-c^2)} \tag{2.1127}$$

and similar equations hold when α or α and β are imaginary. The procedure for computation is as follows. Choose Poisson's ratio, ν, which fixes c. Then choose a value of ω/ω_α, so that α is determined by (2.1125). Equations (2.1127) then have γ as the only variable and a sequence of roots may be computed numerically. To each root γ there corresponds a value of ξb according to (2.1126). Thus, for the given ω/ω_α we have a set of values of ξb. The process is repeated for the same c and for a sufficient number of values of ω/ω_α to enable curves to be drawn. The results of such a computation for are shown in Fig. 2.111. The full lines are for the symmetric modes and the dashed lines are for the antisymmetric modes. The intersection points are the same as the intersection points in Fig. 2.091. Each such point is identified in Fig. 2.111 by a pair of numbers the first of which is the value of m and the second the value of n.

As may be seen, from Fig. 2.101, the nearly horizontal portions of the curves in Fig. 2.111 are due to the coupling of the equivoluminal modes with the lowest dilatational mode. This effect becomes more pronounced as ξb becomes longer; and, in addition, coupling with the higher dilatational modes produces the terrace-like structure illustrated in Fig. 2.112.

Neither Fig. 2.111, nor the analysis thus far, gives any indication of the character of the frequency spectrum at high frequencies and long wave-lengths. From the fact that the simple thickness-modes are solutions of the differential equations and boundary conditions when the wave-length is infinite, it appears appropriate to examine the Rayleigh solution in the neighborhood of these frequencies and long wave-lengths.

We consider, first, the symmetric modes, whose frequencies are determined by (2.116), which may be written in the form

$$4\xi^2 b^2 \alpha b\, \beta b \sin \alpha b \cos \beta b + (\xi^2 b^2 - \beta^2 b^2) \sin \beta b \cos \alpha b = 0 \qquad (2.1128)$$

where

$$\alpha b = \sqrt{\omega^2 b^2 v_1^{-2} - \xi^2 b^2}$$
$$\beta b = \sqrt{\omega^2 b^2 v_2^{-2} - \xi^2 b^2} \qquad (2.1129)$$

We seek solutions in the neighborhood $\xi b \ll 1$ and

$$\omega = \begin{cases} (p+\epsilon)\omega_t\,, & p = 1,3,5,\ldots \\ (q+\epsilon)\omega_s\,, & q = 2,4,6,\ldots \end{cases}, \quad |\epsilon| \ll 1 \qquad (2.1130)$$

where

$$\omega_t = \frac{\pi v_1}{2b}\,, \qquad \omega_s = \frac{\pi v_2}{2b} \qquad (2.1131)$$

Inserting (2.1130) in (2.1129), expanding the radicals and dropping products and powers of ξb and ϵ higher than the second degree, we obtain

$$\alpha b = \begin{cases} \left(\frac{p\pi}{2} + \frac{\pi\epsilon}{2} - \frac{\xi^2 b^2}{p\pi}\right), & p = 1,3,5,\ldots \\ \frac{1}{c}\left(\frac{q\pi}{2} + \frac{\pi\epsilon}{2} - \frac{c^2\xi^2 b^2}{q\pi}\right), & q = 2,4,6,\ldots \end{cases}$$

$$\beta b = \begin{cases} c\left(\frac{p\pi}{2} + \frac{\pi\epsilon}{2} - \frac{\xi^2 b^2}{p\pi c^2}\right), & p = 1,3,5,\ldots \\ \left(\frac{q\pi}{2} + \frac{\pi\epsilon}{2} - \frac{\xi^2 b^2}{q\pi}\right), & q = 2,4,6,\ldots \end{cases} \qquad (2.1132)$$

Then, to the same approximation, we find, for $p = 1,3,5,\ldots$, $q = 2,4,6,\ldots$,

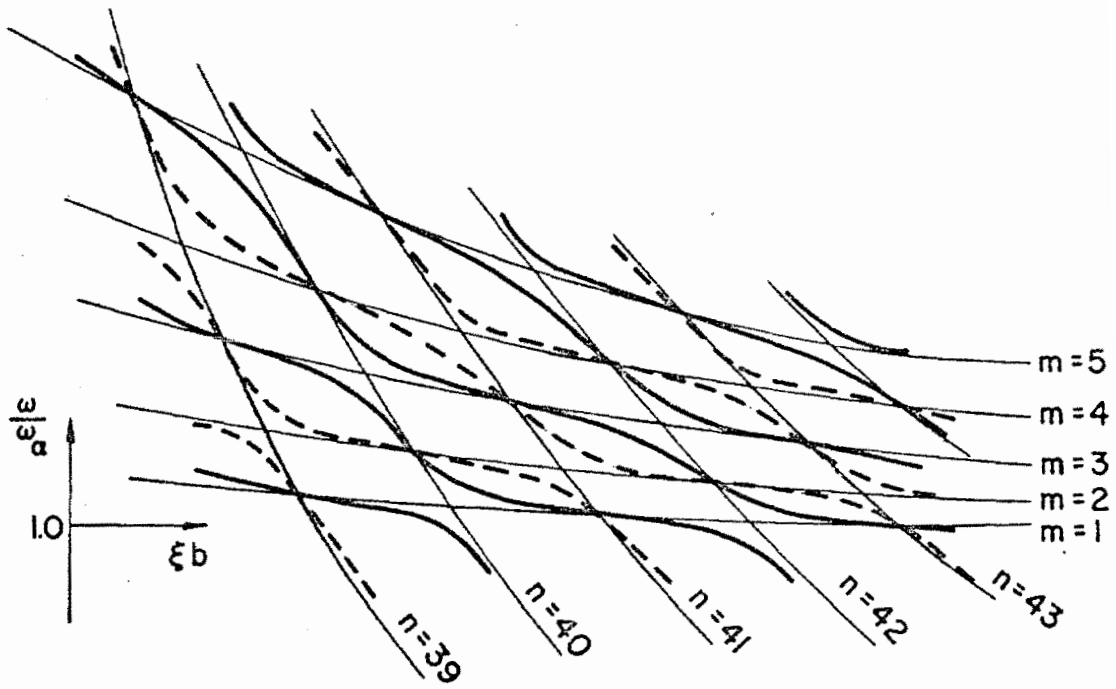

Fig. 2.112

Terrace-like structure of frequency spectrum.

$$\sin \alpha b = \begin{cases} (-1)^{\frac{p-1}{2}} \left(1 - \frac{\pi^2 \epsilon^2}{8}\right) \\ \left(1 - \frac{\pi^2 \epsilon^2}{8c^2}\right) \sin \frac{q\pi}{2c} - \left(\frac{c\xi^2 b^2}{q\pi} - \frac{\pi \epsilon}{2c}\right) \cos \frac{q\pi}{2c} \end{cases}$$

$$\cos \alpha b = \begin{cases} (-1)^{\frac{p-1}{2}} \left(\frac{\xi^2 b^2}{p\pi} - \frac{\pi \epsilon}{2}\right) \\ \left(1 - \frac{\pi^2 \epsilon^2}{8c^2}\right) \cos \frac{q\pi}{2c} + \left(\frac{c\xi^2 b^2}{q\pi} - \frac{\pi \epsilon}{2c}\right) \sin \frac{q\pi}{2c} \end{cases} \qquad (2.1133)$$

$$\sin \beta b = \begin{cases} \left(1 - \frac{\pi^2 c^2 \epsilon^2}{8}\right) \sin \frac{p\pi c}{2} - \left(\frac{\xi^2 b^2}{p\pi c} - \frac{\pi c \epsilon}{2}\right) \cos \frac{p\pi c}{2} \\ (-1)^{\frac{q}{2}} \left(\frac{\pi \epsilon}{2} - \frac{\xi^2 b^2}{q\pi}\right) \end{cases}$$

$$\cos \beta b = \begin{cases} \left(1 - \frac{\pi^2 c^2 \epsilon^2}{8}\right) \cos \frac{p\pi c}{2} + \left(\frac{\xi^2 b^2}{p\pi c} - \frac{\pi c \epsilon}{2}\right) \sin \frac{p\pi c}{2} \\ (-1)^{\frac{q}{2}} \left(1 - \frac{\pi^2 \epsilon^2}{8}\right) \end{cases}$$

On substitution of (2.1132) and (2.1133) in (2.1128) we obtain, to a sufficient approximation,

$$\begin{cases} \frac{8\xi^2 b^2}{p^2 \pi^3} \left(\frac{4}{c^3} \cos \frac{p\pi c}{2} + \frac{p\pi}{4} \sin \frac{p\pi c}{2}\right) - \epsilon \sin \frac{p\pi c}{2} - \epsilon^2 \left(\frac{\pi c}{2} \cos \frac{p\pi c}{2} + \frac{4}{p} \sin \frac{p\pi c}{2}\right) = 0 \\ \frac{8\xi^2 b^2}{q^2 \pi^3} \left(\frac{4}{c} \sin \frac{q\pi}{2c} - \frac{q\pi}{4} \cos \frac{q\pi}{2c}\right) + \epsilon \cos \frac{q\pi}{2c} - \epsilon^2 \left(\frac{\pi}{2c} \sin \frac{q\pi}{2c} - \frac{4}{q} \cos \frac{q\pi}{2c}\right) = 0 \end{cases} \qquad (2.1134)$$

We see that $\xi b \to 0$ as $\epsilon \to 0$. Hence the supposition (2.1130) is confirmed, i.e., the limiting frequencies of the symmetric modes, as $\xi b \to 0$, are the frequencies of the symmetric, simple thickness-stretch and thickness-shear modes. We proceed to find the limiting slopes and curvatures of the curves ω/ω_s vs. ξb.

From (2.1130),

$$\epsilon = \begin{cases} \frac{1}{c} \frac{\omega}{\omega_s} - p \\ \frac{\omega}{\omega_s} - q \end{cases} \qquad (2.1135)$$

Hence, for small ϵ, from (2.1134) and (2.1135),

$$\frac{d(\omega/\omega_s)}{d(\xi b)} = \begin{cases} \frac{16c\xi b}{p^2\pi^3}\left(\frac{p\pi}{4} + \frac{4}{c^3}\cot\frac{p\pi c}{2}\right) \\ \frac{16\xi b}{q^2\pi^3}\left(\frac{q\pi}{4} - \frac{4}{c}\tan\frac{q\pi}{2c}\right) \end{cases} \tag{2.1136}$$

$$\frac{d^2(\omega/\omega_s)}{d(\xi b)^2} = \begin{cases} \frac{16c}{p^2\pi^3}\left(\frac{p\pi}{4} + \frac{4}{c^3}\cot\frac{p\pi c}{2}\right) \\ \frac{16}{q^2\pi^3}\left(\frac{q\pi}{4} - \frac{4}{c}\tan\frac{q\pi}{2c}\right) \end{cases} \tag{2.1137}$$

Accordingly, if

$$\begin{cases} \sin\frac{p\pi c}{2} \neq 0 \;\; ; \; p=1,3,5,\ldots \\ \cos\frac{q\pi}{2c} \neq 0 \;\; ; \; q=2,4,6,\ldots \end{cases} \tag{2.1138}$$

the slopes at $\xi b = 0$ are zero and the curvatures are positive or negative according as

$$\begin{cases} \frac{p\pi}{4} + \frac{4}{c^3}\cot\frac{p\pi c}{2} \gtrless 0 \\ \frac{q\pi}{4} - \frac{4}{c}\tan\frac{q\pi}{2c} \gtrless 0 \end{cases} \tag{2.1139}$$

If, however,

$$\begin{cases} \sin\frac{p\pi c}{2} = 0 \\ \cos\frac{q\pi}{2c} = 0 \end{cases}$$

the corresponding curvatures become infinite and the slopes cannot be determined from (2.1136). In this case, from both of (2.1140), we have

$$c = \frac{q}{p} \quad \begin{cases} q=2,4,6,\ldots \\ p=1,3,5,\ldots \end{cases} \tag{2.1141}$$

Then, inserting (2.1140) and (2.1141) in (2.1134) we find

$$\frac{d(\omega/\omega_s)}{d(\xi b)} = \pm \frac{8}{q\pi^2} \quad , \quad q = 2, 4, 6, \ldots \tag{2.1142}$$

Now, the condition (2.1140), or (2.1141), is the criterion for coincidence of the frequency of a simple, symmetric, thickness-stretch mode with the frequency of a simple, symmetric, thickness-shear mode. Expressed explicitly in terms of elastic constants, we have

$$c = \sqrt{\frac{\lambda+2\mu}{\mu}} = \sqrt{\frac{2(1-\nu)}{1-2\nu}} = \frac{q}{p}$$

or

$$\nu = \frac{q^2-2p^2}{2(q^2-p^2)} \tag{2.1143}$$

For example, $\nu = 1/3$ when $p=1$ and $q=2$; or, alternatively, when $\nu = 1/3$ the lowest symmetric thickness-stretch mode (Fig. 2.031) has the same frequency as the lowest symmetric thickness-shear mode (Fig. 2.032).

The character of the coupled modes as ν passes from below to above is illustrated by the heavy, full lines in Fig. 2.113. We shall examine, in detail, the behavior of the curve corresponding to $p=1$ as it rises in the spectrum with increasing Poisson's ratio. When $\nu = 0.25$, the curve for the second symmetric mode in Fig. 2.113(a) approaches $\omega/\omega_s = \sqrt{3}$ as $\xi b \to 0$. This is the frequency of the symmetric, simple thickness-stretch mode $p=1$. From the first of (2.1136) the slope is zero at $\xi b = 0$ and, from the first of (2.1137), with $p=1$, the curvature at $\xi b = 0$ is negative. As ν approaches $1/3$, the slope remains zero, the curvature approaches negative infinity and the frequency approaches $\omega/\omega_s = 2$, i.e., the frequency of the symmetric, simple thickness-shear mode $q=2$. At $\nu = 1/3$, the slope, from (2.1142), with $q=2$, is $-4/\pi^2$. As ν exceeds $1/3$ the slope of the curve corresponding to $p=1$ switches from $-4/\pi^2$ to $+4/\pi^2$ and then to zero slope and positive curvature. The curve corresponding to $p=1$ has now become the third

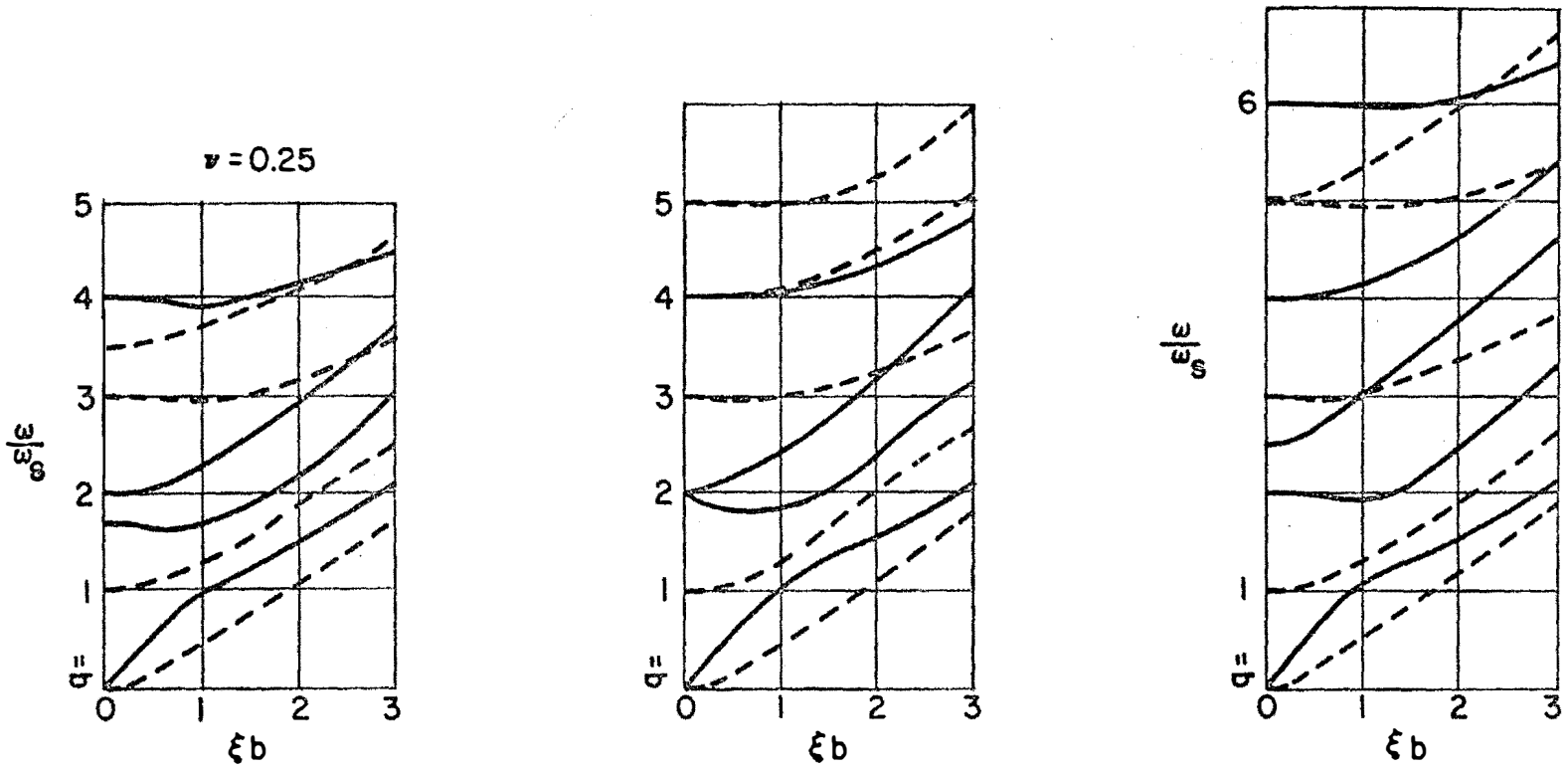

Fig. 2.113

Influence of Poisson's ratio on the frequency spectrum of an infinite, isotropic plate with free faces.

symmetric mode, having passed above the curve corresponding to the symmetric thickness-shear mode $q=2$. This is illustrated, in Fig. 2.113, for $\nu=0.40$, for which ω/ω_s is about 2.5 for $p=1$ and $\xi b=0$. As Poisson's ratio increases above 0.40, the curve corresponding to $p=1$ approaches the curve corresponding to $q=4$ (at $\omega/\omega_s=4$). Its slope at $\xi b=0$ remains zero, but its curvature diminishes, passing through zero at $\nu=0.46$. (This is the second root of the equation obtained by setting the first of (2.1137) equal to zero. The first root occurs at $\nu=-0.5$.) Then, as $\nu\to 7/15$ the curvature again approaches negative infinity and the cycle is repeated as the curve corresponding to $p=1$ passes the curve corresponding to $q=4$. This time, however, the switch of slope is from $-1/\pi^2$ to $+1/\pi^2$. The curve corresponding to $p=1$ passes through a similar cycle each time ν increases through a value given by (2.1143) with $p=1$ and $q=2,4,6,\ldots$. This is illustrated in Fig. 2.114 for the first four cycles. (It is to be noted that the groups of curves in Fig. 2.114 have been shifted to a common ordinate at $\xi b=0$.) A similar phenomenon occurs with each of the curves corresponding to $p=1,3,5,\ldots$ provided that the value of ν given by (2.1143) lies in the range

$$-1 \ll \nu \leq \tfrac{1}{2} \qquad (2.1144)$$

For example, the curve corresponding to $p=3$ never falls below the curve corresponding to $q=2$, since, in this case (2.1143) gives $\nu=7/5$. That is, the simple thickness-stretch mode $p=3$ always has a higher frequency than the simple thickness-shear mode $q=2$ (see Figs. 2.031 and 2.032). However, $p=3$ passes $q=4$ at $\nu=-1/7$; $q=6$ at $\nu=1/3$, etc.

Thus far, we have made use of only the first of each of the pairs of equations (2.1134) to (2.1140). This is because we have fixed attention on a single mode corresponding to $p=$ constant as it passes modes corresponding to $q=$ constant. If we fix attention on a mode corresponding to $q=$ constant,

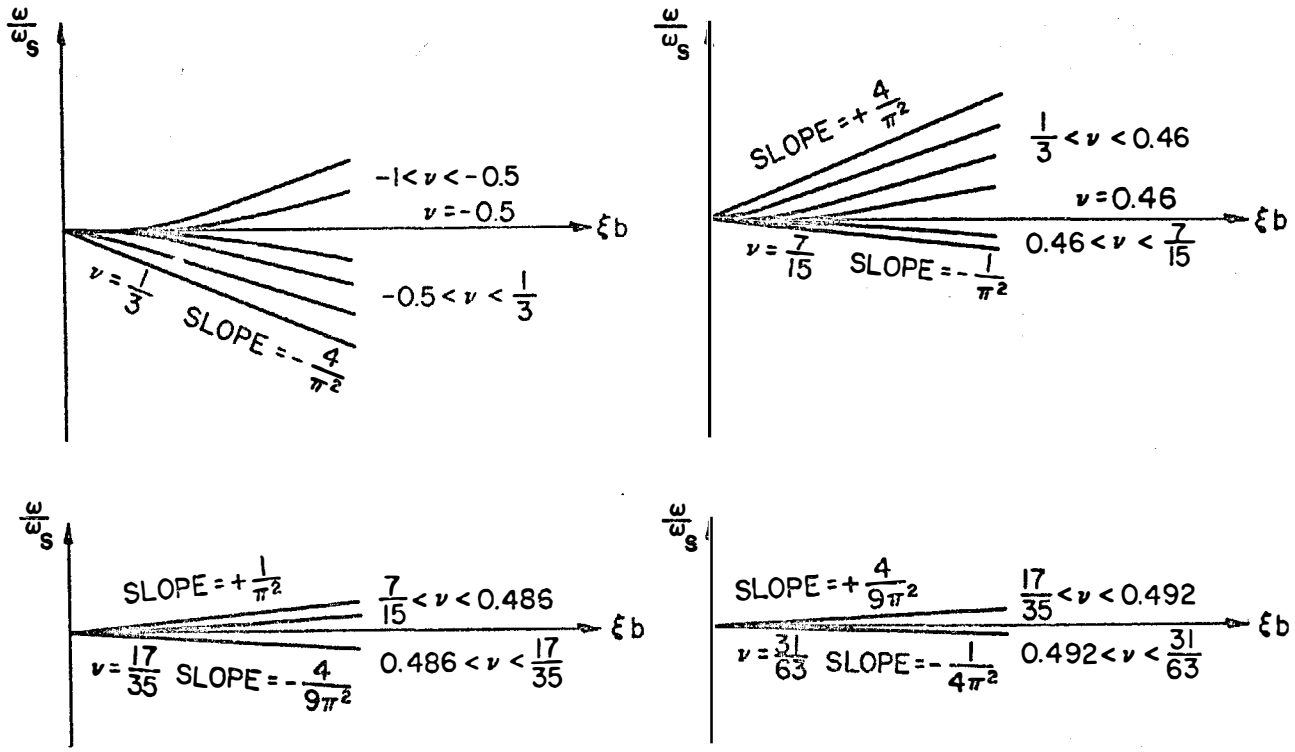

Fig. 2.114

Initial curvature and slope of a spectral curve as influenced by Poisson's ratio.

the second of each of the pairs of equations shows that a similar phenomenon occurs when the curve corresponding to q = constant is passed by each of the modes corresponding to p = constant.

We turn, now, to a consideration of the antisymmetric modes, whose frequencies are determined by (2.118) which may be written in the form

$$4\xi^2b^2\,\alpha b\,\beta b\sin\beta b\cos\alpha b+(\xi^2b^2-\beta^2b^2)^2\sin\alpha b\cos\beta b=0 \qquad (2.1145)$$

This time we seek solutions in the neighborhood $\xi b \ll 1$ and

$$\omega=\begin{Bmatrix}(p+\epsilon)\omega_t\,,\ p=2,4,6,\dots\\(q+\epsilon)\omega_s\,,\ q=1,3,5,\dots\end{Bmatrix},\ |\epsilon|\ll 1 \qquad (2.1146)$$

To the second degree in ξb and ϵ we find

$$\alpha b=\begin{cases}\left(\frac{p\pi}{2}+\frac{\pi\epsilon}{2}-\frac{\xi^2b^2}{p\pi}\right),\ p=2,4,6,\dots\\ \frac{1}{c}\left(\frac{q\pi}{2}+\frac{\pi\epsilon}{2}-\frac{c^2\xi^2b^2}{q\pi}\right),\ q=1,3,5,\dots\end{cases}$$

$$\beta b=\begin{cases}c\left(\frac{p\pi}{2}+\frac{\pi\epsilon}{2}-\frac{\xi^2b^2}{p\pi c^2}\right),\ p=2,4,6,\dots\\ \left(\frac{q\pi}{2}+\frac{\pi\epsilon}{2}-\frac{\xi^2b^2}{q\pi}\right),\ q=1,3,5,\dots\end{cases} \qquad (2.1147)$$

$$\sin\alpha b = \begin{cases} (-1)^{\frac{p}{2}}\left(\frac{\pi\epsilon}{2} - \frac{\xi^2 b^2}{p\pi}\right) \\ \left(1-\frac{\pi^2\epsilon^2}{8c^2}\right)\sin\frac{q\pi}{2c} - \left(\frac{c\xi^2 b^2}{q\pi} - \frac{\pi\epsilon}{2c}\right)\cos\frac{q\pi}{2c} \end{cases}$$

$$\cos\alpha b = \begin{cases} (-1)^{\frac{p}{2}}\left(1-\frac{\pi^2\epsilon^2}{8}\right) \\ \left(1-\frac{\pi^2\epsilon^2}{8c^2}\right)\cos\frac{q\pi}{2c} + \left(\frac{c\xi^2 b^2}{q\pi} - \frac{\pi\epsilon}{2c}\right)\sin\frac{q\pi}{2c} \end{cases}$$

$$\sin\beta b = \begin{cases} \left(1-\frac{\pi^2 c^2\epsilon^2}{8}\right)\sin\frac{p\pi c}{2} - \left(\frac{\xi^2 b^2}{p\pi c} - \frac{\pi c\epsilon}{2}\right)\cos\frac{p\pi c}{2} \\ (-1)^{\frac{q-1}{2}}\left(1-\frac{\pi^2\epsilon^2}{8}\right) \end{cases}$$

$$\cos\beta b = \begin{cases} \left(1-\frac{\pi^2 c^2\epsilon^2}{8}\right)\cos\frac{p\pi c}{2} + \left(\frac{\xi^2 b^2}{p\pi c} - \frac{\pi c\epsilon}{2}\right)\sin\frac{p\pi c}{2} \\ (-1)^{\frac{q-1}{2}}\left(\frac{\xi^2 b^2}{q\pi} - \frac{\pi\epsilon}{2}\right) \end{cases} \qquad (2.1148)$$

Then (2.1145) becomes

$$\begin{cases} \frac{8\xi^2 b^2}{p^2\pi^3}\left(\frac{4}{c^3}\sin\frac{p\pi c}{2} - \frac{p\pi}{4}\cos\frac{p\pi c}{2}\right) + \epsilon\cos\frac{p\pi c}{2} - \epsilon^2\left(\frac{\pi c}{2}\sin\frac{p\pi c}{2} - \frac{4}{p}\cos\frac{p\pi c}{2}\right) = 0 \\ \frac{8\xi^2 b^2}{q^2\pi^3}\left(\frac{4}{c}\cos\frac{q\pi}{2c} + \frac{q\pi}{4}\sin\frac{q\pi}{2c}\right) - \epsilon\sin\frac{q\pi}{2c} - \epsilon^2\left(\frac{\pi}{2c}\cos\frac{q\pi}{2c} + \frac{4}{q}\sin\frac{q\pi}{2c}\right) = 0 \end{cases} \qquad (2.1149)$$

from which

$$\frac{d(\omega/\omega_3)}{d(\xi b)} = \begin{cases} \frac{16c\xi b}{p^2\pi^3}\left(\frac{p\pi}{4} - \frac{4}{c^3}\tan\frac{p\pi c}{2}\right) \\ \frac{16\xi b}{q^2\pi^3}\left(\frac{q\pi}{4} + \frac{4}{c}\cot\frac{q\pi}{2c}\right) \end{cases} \qquad (2.1150)$$

$$\frac{d^2(\omega/\omega_3)}{d(\xi b)^2} = \begin{cases} \frac{16c}{p^2\pi^3}\left(\frac{p\pi}{4} - \frac{4}{c^3}\tan\frac{p\pi c}{2}\right) \\ \frac{16}{q^2\pi^3}\left(\frac{q\pi}{4} + \frac{4}{c}\cot\frac{q\pi}{2c}\right) \end{cases} \qquad (2.1151)$$

Accordingly, if

$$\begin{cases} \cos\frac{p\pi c}{2} \neq 0 \ , \quad p=2,4,6,\ldots \\ \sin\frac{q\pi}{2c} \neq 0 \ , \quad q=1,3,5,\ldots \end{cases} \tag{2.1152}$$

the slopes at $\xi b=0$ are zero and the curvatures are positive or negative according as

$$\begin{cases} \frac{p\pi}{4} - \frac{4}{c^3}\tan\frac{p\pi c}{2} \gtrless 0 \\ \frac{q\pi}{4} + \frac{4}{c}\cot\frac{q\pi}{2c} \gtrless 0 \end{cases} \tag{2.1153}$$

If, however,

$$\begin{cases} \cos\frac{p\pi c}{2} = 0 \\ \sin\frac{q\pi}{2c} = 0 \end{cases} \tag{2.1154}$$

so that

$$c = \frac{q}{p} \begin{cases} q=3,5,\ldots \\ p=2,4,6,\ldots \end{cases} \tag{2.1155}$$

the curvatures are infinite and the slopes, from (2.1149) are

$$\frac{d(\omega/\omega_s)}{d(\xi b)} = \pm\frac{8}{q\pi^2} \ , \quad q=3,5,\ldots \tag{2.1156}$$

Thus, the behavior of the antisymmetric modes is similar to that of the symmetric modes, but with one important exception. It will be observed that (2.1154)-(2.1156) do not hold for $q=1$. This is because ν is limited to the range

$$-1 \ll \nu \ll \tfrac{1}{2}$$

so that

$$\frac{2}{\sqrt{3}} \ll c \ll \infty$$

Hence, even the smallest value of p (i.e., $p=2$) does not bring c within the allowable range. This is to say that the frequency of the lowest, antisymmetric, simple thickness-stretch mode (Fig. 2.031, $p=2$) is always higher than the frequency of the lowest antisymmetric, simple thickness-shear mode (Fig. 2.032, $q=1$). Hence the coupled mode corresponding to $q=1$ never goes through the cycle of change of sign of curvature. This is illustrated by the dashed curves in Fig. 2.113. The second antisymmetric mode always has the same character while Poisson's ratio varies. The third antisymmetric mode, however, does go through the cycle, since the frequency of the lowest, antisymmetric, simple thickness-stretch mode is lower than the frequency of the second antisymmetric thickness-shear mode (Fig. 2.032, $q=3$) if $\nu < 1/10$. In Fig. 2.113 the lowest value of Poisson's ratio for which the spectrum is illustrated is $\nu = 0.25$, so that in (a) the curve corresponding to $p=2$ (the fourth antisymmetric mode) is already above that corresponding to $q=3$. Its ordinate at $\xi b = 0$ is $2\sqrt{3}$, i.e., about 3.5. The next value above $\nu = 1/10$ for which coincidence occurs is $\nu = 17/42$ (obtained from (2.1143) with $p=2$, $q=5$). This is slightly above $\nu = 0.40$, for which Fig. 2.113(c) is plotted. Hence the fourth and fifth antisymmetric modes are shown just prior to their meeting point at $\omega/\omega_s = 5$.

2.12 Three-Dimensional Coupled Dilatational and Equivoluminal Modes in an Infinite Isotropic Plate with Free Faces

The solution given in Section 2.11 may be extended to include phase reversals in the x_3-direction.

In (1.077) we take, for the potentials of the dilatation and rotation,

$$\varphi = f(x_2)\sin\xi \qquad \zeta x_3\, e^{i\omega t}$$
$$H_1 = h_1(x_2)\sin\xi x_1 \cos\zeta x_3\, e^{i\omega t}$$
$$H_2 = h_2(x_2)\cos\xi x_1 \cos\zeta x_3\, e^{i\omega t} \qquad (2.121)$$
$$H_3 = h_3(x_2)\cos\xi x_1 \sin\zeta x_3\, e^{i\omega t}$$

sfy the equations of ? (1.078) and (1.0710) are satisfied,

i.e., if

$$\xi h_1 + h_2' + \zeta h_3 = 0$$
$$f'' + \alpha^2 f = 0 \qquad (2.122)$$
$$h_j'' + \beta^2 h_j = 0, \quad j = 1,2,3.$$

where

$$\alpha^2 + \xi^2 + \zeta^2 = \omega^2/V_1^2$$
$$\beta^2 + \xi^2 + \zeta^2 = \omega^2/V_2^2 \qquad (2.123)$$

Thus,

$$f = A\sin\alpha x_2 + B\cos\alpha x_2$$
$$h_j = C_j \sin\beta x_2 + D_j \cos\beta x_2, \quad j = 1,2,3. \qquad (2.124)$$

ıd, for the components of displacement and for the components of

›lanes x_2 = constant,

$$u_1 = (\xi f + h_3' + \zeta h_2)\cos\xi x_1 \sin\zeta x_3\, e^{i\omega t}$$
$$u_2 = (f' - \zeta h_1 + \xi h_3)\sin\xi x_1 \sin\zeta x_3\, e^{i\omega t} \qquad (2.125)$$
$$u_3 = (\zeta f - \xi h_2 - h_1')\sin\xi x_1 \cos\zeta x_3\, e^{i\omega t}$$

$$= \mu[(\xi^2+\zeta^2-\beta^2)f + 2(\xi h_3' - \zeta h_1')]\sin\xi x_1 \sin\zeta x_3\, e^{i\omega t}$$
$$= \mu[2\zeta f' - (\zeta^2-\beta^2)h_1 - \xi h_2' + \xi\zeta h_3]\sin\xi x_1 \cos\zeta x_3\, e^{i\omega t} \qquad (2.126)$$
$$= \mu[2\xi f' - \xi\zeta h_1 + \zeta h_2' + (\xi^2-\beta^2)h_3]\cos\xi x_1 \sin\zeta x_3\, e^{i\omega t}$$

e symmetric modes we take, from (2.124),

$$f = B\cos\alpha x_2 \qquad h_1 = C_1 \sin\beta x_2$$
$$h_2 = D_2 \cos\beta x_2 \qquad (2.127)$$
$$h_3 = C_3 \sin\beta x_2$$

Then, the first of (2.122) and the boundary conditions $T_{22} = T_{23} = T_{12} = 0$ on $x_2 = \pm b$ require

$$\begin{array}{cccc} \xi C_1 & -\beta D_2 & +\zeta C_3 & = 0 \\ (\xi^2+\zeta^2-\beta^2)B\cos\alpha b & -2\zeta\beta C_1\cos\beta b & +2\xi\beta C_3\cos\beta b & = 0 \\ -2\zeta\alpha B\sin\alpha b & -(\zeta^2-\beta^2)C_1\sin\beta b + \xi\beta D_2\sin\beta b & +\xi\zeta C_3\sin\beta b & = 0 \\ -2\xi\alpha B\sin\alpha b & -\xi\zeta C_1\sin\beta b & -\zeta\beta D_2\sin\beta b + (\xi^2-\beta^2)C_3\sin\beta b & = 0 \end{array} \qquad (2.128)$$

When the determinant of (2.128) is set equal to zero we obtain

$$\frac{\tan\beta b}{\tan\alpha b} = -\frac{4\alpha\beta(\xi^2+\zeta^2)^2}{(\xi^2+\zeta^2-\beta^2)^2} \qquad (2.129)$$

Similarly, for the antisymmetric modes, we obtain

$$\frac{\tan\beta b}{\tan\alpha b} = -\frac{(\xi^2+\zeta^2-\beta^2)^2}{4\alpha\beta(\xi^2+\zeta^2)^2} \qquad (2.1210)$$

It will be observed that (2.129) and (2.1210) are the same as (2.116) and (2.118) except that $\xi^2+\zeta^2$ takes the place of ξ^2. (This was pointed out by Rayleigh, 1889.) Hence, all the results obtained for the problem of plane strain, treated in Section 2.11, hold for the three-dimensional case if the wave-number, ξ, in Section 2.11, is replaced by $\sqrt{\xi^2+\zeta^2}$. In particular, the frequency spectra, depicted in all the Figures in Section 2.11, apply to the present case if this substitution is made in the coordinates.

2.13 Solutions in Cylindrical Coordinates

The solutions given in Sections 2.07 and 2.11 have their counterparts in cylindrical coordinates (Goodman, 1951). We refer the plate to the cylindrical coordinate system r, θ, z and take the faces at $z = \pm b$. The vector potential (H_1, H_2, H_3) is resolved into cylindrical components (H_r, H_θ, H_z) and we consider the axially symmetric case, in which $H_r = H_z = 0$ and H_θ and φ are independent of θ. Then (1.077) become, in cylindrical coordinates,

$$\begin{aligned} u_r &= \frac{\partial \varphi}{\partial r} - \frac{\partial H_\theta}{\partial z} \\ u_\theta &= 0 \\ u_z &= \frac{\partial \varphi}{\partial z} + \frac{\partial H_\theta}{\partial r} + \frac{H_\theta}{r} \end{aligned} \tag{2.131}$$

and (1.0710) become

$$\begin{aligned} V_1^2 \nabla^2 \varphi &= \ddot{\varphi} \\ V_2^2 (\nabla^2 H_\theta - r^{-2} H_\theta) &= \ddot{H}_\theta \end{aligned} \tag{2.132}$$

Equations (2.13$\not{7}$) have solutions

$$\begin{aligned} \varphi &= f(z) J_0(\xi r)\, e^{i\omega t} \\ H_\theta &= h(z) J_1(\xi r)\, e^{i\omega t} \end{aligned} \tag{2.133}$$

where J_0 and J_1 are Bessel functions and, as before,

$$\begin{aligned} f'' + \alpha^2 f &= 0 \\ h'' + \beta^2 h &= 0 \\ \alpha^2 + \xi^2 &= \omega^2 / V_1^2 \\ \beta^2 + \xi^2 &= \omega^2 / V_2^2 \end{aligned} \tag{2.134}$$

Then

$$
\begin{aligned}
u_r &= -(\xi f + h')\, J_1(\xi r)\, e^{i\omega t} \\
u_z &= (f' + \xi h)\, J_0(\xi r)\, e^{i\omega t} \\
T_{zz} &= \lambda\Delta + 2\mu \frac{\partial u_r}{\partial r} = \mu[(\xi^2 - \beta^2) f + 2\xi h']\, J_0(\xi r)\, e^{i\omega t} \\
T_{rz} &= \mu\left(\frac{\partial u_r}{\partial z} + \frac{\partial u_z}{\partial r}\right) = -\mu[2\xi f' + (\xi^2 - \beta^2)]\, J_1(\xi r)\, e^{i\omega t}
\end{aligned}
\qquad (2.135)
$$

Since the quantities in brackets in the expressions for T_{zz} and T_{rz} are the same as those in T_{22} and T_{12} in (2.068), and since α, β, ξ and ω are related in the same way as before, all the conclusions regarding frequencies of vibration, which were reached in the case of rectangular coordinates, apply also to the case of cylindrical coordinates. Figs. 2.091 and 2.092 give the frequency spectra for a plate held between smooth, rigid faces and Figs. 2.111, 2.112 and 2.113 give the frequency spectra for a plate with free faces.

Equivoluminal modes also exist, as may be seen by setting $f = 0$, $\xi^2 = \beta^2$ and $h'(\pm b) = 0$ in (2.135). In this case T_{rr} is proportional to $J_1'(\xi r)$ and hence the plate breaks up into traction-free rings bounded by cylindrical surfaces $J_1'(\xi r) = 0$. As before, planes z = constant are free of traction at intervals $2b/n$.

Three-dimensional solutions in cylindrical coordinates, analogous to those in Section 2.12, may be obtained by retaining H_r and H_z and setting all functions proportional to $\cos n\theta$ or $\sin n\theta$.

2.14 Additional Boundaries

In Sections 2.11 and 2.12, dealing with coupled dilatational and equivoluminal modes in isotropic plates with free faces, we saw that, for either the symmetric or antisymmetric case, there is an infinite number of modes of vibration for each ratio of thickness to wave-length. Each of these modes can exist, in an infinite plate, independently of all the others. This is the

analogue of the independence of dilatational and equivoluminal modes in a body with all its dimensions infinite. Now, considering, for example, a single symmetric mode in a plate with free faces, we find that at intervals π/ξ along x_1 (at every crest and trough) boundary conditions $u_1 = T_{13} = T_{12} = 0$ are satisfied. This is the analogue of the case of smooth rigid boundaries ($u_2 = T_{23} = T_{12} = 0$ on $x_2 = \pm b$) treated in Section 2.09. In that case we saw that relaxation of the condition $u_2 = 0$ to $T_{22} = 0$ resulted in coupling of equivoluminal and dilatational modes. In an analogous manner the relaxation of the boundary conditions $u_1 = 0$ to $T_{11} = 0$, on planes x_1 = constant, of a plate with free faces $x_2 = \pm b$, results in the coupling of the infinity of modes of the type described in Section 2.11 or 2.12. Hence, with the exception of modes of the type treated in Section 2.07, the modes of vibration of a plate, with more free boundaries than the free faces, are not expressible in closed form. This leads to major computational difficulties because the equations which then determine the frequencies and mode-shapes, analogous to (2.115) and (2.116), contain an infinite number of terms. The same difficulty occurs, of course, with crystal plates; and in these there are the additional complications that, in general, the relation between wave-number and frequency, analogous to (2.066), is determined by a cubic equation and symmetric and antisymmetric motions are coupled. Thus, for both isotropic and crystal plates it is convenient to have available approximate equations which contain only a finite number of modes of the type encountered in Sections 2.11 and 2.12. Such approximations are made, of course, at the expense of limiting the applicability of the equations to certain classes of modes and ranges of frequencies and wave-lengths.